REPUBLIC OF TURKEY
YILDIZ TECHNICAL UNIVERSITY
GRADUATE SCHOOL OF NATURAL AND APPLIED SCIENCES

H_∞ CONTROL AND MATHEMATICAL MODELING OF A QUARTER-CAR SYSTEM VIA NON-PARAMETRIC APPROACH

CANALP BELGÜTAY

MSc. THESIS
DEPARTMENT OF CONTROL AND AUTOMATION ENGINEERING
PROGRAM OF CONTROL AND AUTOMATION ENGINEERING

ADVISER
ASST. PROF. AKIN DELİBAŞI

İSTANBUL, 2015

REPUBLIC OF TURKEY

YILDIZ TECHNICAL UNIVERSITY

GRADUATE SCHOOL OF NATURAL AND APPLIED SCIENCES

H_∞ CONTROL AND MATHEMATICAL MODELING OF A QUARTER-CAR SYSTEM VIA NON-PARAMETRIC APPROACH

A thesis submitted by Canalp BELGÜTAY in partial fulfillment of the requirements for the degree of **MASTER OF SCIENCE** is approved by the committee on 29.04.2015 in Department of Control and Automation Engineering, Control and Automation Program.

Thesis Adviser

Asst. Prof. Akın Delibaşı

Yıldız Technical University

Approved By the Examining Committee

Asst. Prof. Akın Delibaşı

Yıldız Technical University _____

Professor Alpaslan Parlakçı

Istanbul Bilgi University _____

Asst. Prof. Janset Daşdemir

Yıldız Technical University _____

ACKNOWLEDGEMENTS

Studying in this department has given me a chance to blend my mechanical knowledge with electronic control systems. It was a useful experience that will contribute to me in my future life, career and my academic future.

I would like to extend my gratitude to my advisor, Asst. Prof. Akın DELİBAŞI for his mentorship and sympathy over the last 2 years. His efforts and contributions on me are very valuable and dear. I also thank him for the valuable conversations, discussions and advices I had through our relationship.

The system that was used in this thesis is a linear actuated quarter car suspension system which is developed by the TÜBİTAK project number 108E089. I would like to hereby present my thanks to the project executive Assoc. Prof. Dr. İbrahim Beklan KÜÇÜKDEMİRAL. I also thank to Ass. Bilal EROL for helping me work in the laboruatory.

I also would like to thank my life-long friends Baran ÖZBEK and Berk ERGUN for their constant support.

March, 2015

Canalp BELGÜTAY

TABLE OF CONTENTS

LIST OF SYMBOLS

$A(q)$	Output polynomial for a simple representation for model structures
a	A variable for model structures
B	A variable for model structures
$B(q)$	Input polynomial for a simple representation for model structures
$C(q)$	Box-Jenkins model numerator polynomial for the error
c	Damping constant
c_b	Damping constant of the body
c_c	Critical damping coefficient
c_s	Damping ratio of the sprung mass
c_t	Tire dissipation
$D(q)$	Box-Jenkins model denumerator polynomial for the error
E	Energy
$e(t)$	Disturbance at a time
F	Force
F_a	Actuator force
$F(q)$	The polynomial used to simplify model structures
G	Input to output factor in LTI models
H	Disturbance to output factor in LTI models
f_0	Amplitude of the sinusoidal input for the free vibration system
K	Feedback
KE	Kinetic energy
k	Spring constant
k_1	First spring constant
k_2	Second spring constant
k_b	Spring constant of the body mass
k_e	Equivalent spring constant
k_s	Spring constant of the sprung mass
k_t	Spring constant of the tire
m	Mass
m_b	Body mass
m_s	Mass of the sprung mass
m_u	Mass of the unsprung mass
m_w	Suspension mass

n_a	Number of poles of model structures
n_b	Number of zeros of model structures
n_k	Time delay for model structures
PE	Potential energy
PE_1	First spring potential energy
PE_2	Second spring potential energy
r	Ratio of operating frequency and natural frequency
t	Time
TF	Transfer function
TR	Transmissibility
TR_f	Force transmissibility
TR_d	Displacement transmissibility
u	Sinusoidal input for the free vibration system
$u(t-n_k)$	Delayed input for model structures
V_a	Velocity of the actuator
x	Displacement
x_b	Displacement of the body mass
x_g	Displacement of the road
x_h	Homogeneous solution
x_p	Particular solution
x_r	Road displacement in the real system
x_s	Car body displacement in the real system
x_u	Suspension displacement in the real system
x_w	Displacement of the suspension mass
$y(t)$	Current output of model structures
$y(t-k)$	Past outputs of model structures
y	Control output
z	Performance output
ζ	Damping ratio
ζ_s	Damping ratio for sprung mass
ζ_u	Damping ratio for unsprung mass
φ	Phase angel
ω	Operation frequency
ω_0	Frequency of the sinusoidal input for the free vibration system
ω_n	Natural frequency
ω_{n1-2}	First and second natural frequency

LIST OF ABBREVIATIONS

DOF	Degree of freedom
GUI	Graphical user interface
LPV	Linear parameter varying
MIMO	Multi input- multi output
PID	Proportional-integral-derivative
SDP	Semi- definite programming
SISO	Single input- single output
TR	Transmissibility ratio
TÜBİTAK	The scientific and technological research council of Turkey

LIST OF FIGURES

Page

LIST OF TABLES

Page

ABSTRACT

H_∞ CONTROL AND MATHEMATICAL MODELING OF A QUARTER-CAR SYSTEM VIA NON-PARAMETRIC APPROACH

Canalp BELGÜTAY

Department of Control and Automation Engineering

MSc. Thesis

Adviser: Asst. Prof. Akın Delibaşı

The experimental system that is used in this work is a custom-made MIMO electro-mechanical system which is constructed to be used in a project of The Scientific and Technological Research Council of Turkey (Number: 108E089). This system represents an active suspension system. Modeling and control applications are done for this system while taking the passenger comfort in an active suspension as the engineering problem.

Initially passive suspensions, semi-active suspensions and active suspensions are examined and their mathematical models are presented. The mechanical characteristics of an active suspension's elements are explained. In the light of these information, characteristics of a spring-damper-mass mechanical system are inspected. Natural frequency and damping ratio concepts are reviewed. The mathematical modeling is done by using the Lagrange energy method and ensured by the modeling method which is based on Newton's second law.

It is seen that the real parameters are different than the known label ones. At this point non-parametric system identification methods are included in order to tune these values. Frequency and transient response characteristics are gathered from the experimental system to gain an insight of it. Frequency response characteristics are found by a set of sine wave tests. A Bode-like graphic is presented and the natural frequency locations and damping effects are shown on it. As a result of applying these non-parametric methods, a modified mathematical model is found.

A black-box parametric system modeling is done with the help of MATLAB's system identification toolbox and a 4^{th} order state-space structured model is found. The required data are needed to be used in the parametric system identification algorithms and gathered from the experimental system by an experiment.

The validities of the modified mathematical model and black-box model are compared and secured by checking the output results with the experimental system.

In the control section, initially H_∞ norm of a system and H_∞ control theory are explained. Then H_∞ controllers are calculated for these three models (mathematical, tuned mathematical, black-box). With H_∞ controllers, the peak gains of a system are aimed to be reduced. The performance output is taken as the sprung mass acceleration and their peaks are a crucial factor that effects the passenger comfort in a vehicle. In the simulations, it is seen that the H_∞ controller successfully reduce the peaks of the performance output for each model. However there are some mechanical and electronic limitations for the experimental system and two of the calculated controllers clearly override them. The control law should be supplying a saturation that varies in the boundary of the actuator limits. The controller which is calculated for the black-box model satisfies the both limits and it is applied on the experimental system.

Before starting the experiments, a second-order filter is designed and added to the performance output in order to apmlify certain frequencies, thus a more realistic behaviour is acquired. Experiments are done on the experimental system and it is seen that the H_∞ norm of the experimental system performance output is reduced.

The simulations and experiments are done by using a randomized sine-wave sum input that represent a road test surface.

Key words: Quarter car, modeling, electro-mechanical, H_∞ control, non-parametric system identification methods, parametric system identification methods,

ÖZET

Çeyrek taşıt sisteminin parametrik olmayan yaklaşımla modellenmesi ve $\mathbf{H}_\infty$ kontrolü

Canalp BELGÜTAY

Kontrol ve Otomasyon Mühendisliği Anabilim Dalı

Yüksek Lisans Tezi

Tez Danışmanı: Yrd. Doç. Dr. Akın DELİBAŞI

Bu tezde kullanılan deneysel sistem 108E089 numaralı TÜBİTAK projesi için geliştirilmiş olan çok girişli çok çıkışlı bir elektro mekanik sistemdir. Bu sistem bir aktif süspansiyon sistemini temsil etmektedir. Yolcu komfor sorunu bir mühendislik problemi alınarak bu sistemin modellenmesi ve kontrol uygulamaları yapılmıştır.

Öncelile pasif süspansiyonlar, yarı-aktik süspansiyonlar ve aktif süspansiyonlar ve onların matematik modelleri gösterilmiştir. Bir aktif süspansiyon sisteminin elemanlarının mekanik karakteristikleri açıklanmıştır. Bu bilgilerin ışığında yay-damper-kütle mekanik sisteminin karakteristikleri incelenmiştir. Doğal frekans ve sönümleme oranı kavramları gözden geçirilmiştir. Matematiksel modelleme Lagrange enerji metodları kullanılarak yapıldı ve Newton'ın ikinci yasasını kullanarak yapılan modelleme metodu ile sağlaması yapılmıştır.

Görülmüştürki sistemin gerçek parametreleri bilinen etiket değerlerinden farklıdır. Bu noktada parametrik olmayan sistem tanımlama metodları bu parametreleri düzeltmek için çalışmaya dahil edilmiştir. Deneysel sistemden darbe ve frekans cevabı karakteristikleri alınıp bir anlayış kazandırılmıştır. Frekans cevabı karakteristikleri bir dizi sinüs testi yapılarak bulunmuştur. Bir Bode-tipi grafik çizilip doğal frekansların yerleri ve sönümleme etkileri gözlemlenmiştir. Bu metodların sonucunda modifiye edilmiş bir matematiksel model bulunmuştur.

MATLAB'ın sistem tanımlama araç kutusu ile 4. Dereceden durum uzayı yapısında bir kara-kutu modeli çıkarılmıştır. Gerekli veriler sistemden parametrik sistem tanımlama algoritmalarında kullanılmak için çok girişli çok çıkışlı olarak toplanmıştır.

Parametreleri ayarlanmış matematiksel modelin ve kara-kutu modelinin geçerlilikleri deneysel sistemin cevabı ile kontrol edilerek garanti altına alınmıştır.

Kontrol bölümünde, öncelikle bir sistemin H_∞ normu ve H_∞ kontrol teorisi açıklanmıştır. Sonrasında bu üç model (matematiki modifiye edilmiş matematik, kara-kutu) için H_∞ kontrolcüler tasarlanmıştır. Bir H_∞ kontrolcüler ile bir sistemdeki kazanç uç noktalarının düşürülmesi amaçlanmaktadır. Performans çıkışı üst kütlenin ivmesi olarak alınmıştır ve bu çıkışın kazanç uç noktaları bir araçtaki yolcuların komforunu etkileyen kritik bir faktördür. Simülasyonlarda görülmüştürki, H_∞ kontrolcüler her model için başarılı bir şekilde sistemin performans çıkışı kazanç tepelerini indirmektedir. Ancak deneysel sistem için göz önünde bulundurulması gereken bazı mekanik ve elektronik limitler vardır ve bulunan üç kontrolcüden ikisi bu sınırları bariz bir şekilde aşmaktadır. Bunun için eyleyicinin limitleri dahilinde kalacak şekilde satürasyon sağlayan bir kontrol uygulaması gerekmektedir. Kara-kutu modeli için tasarlanan kontrolcü iki limitide sağlamaktadır ve bu kontrolcü deneysel sistem üzerinde uygulanmıştır.

Deneylere başlamadan önce, ikinci dereceden bir filtre tasarlanarak belli frekansları yükseltmek adına performans çıkışına eklenmiştir, bu sayede daha gerçekçi bir davranış elde edilmiştir. Deneyler gerçek sistemde yapıldığında sistemin performans çıkışının H_∞ normunun düşürüldüğü görülmüştür.

Simülasyonlar ve deneyler değerleri rasgele atanmış olan sinüs dalgalarının toplamıyla elde edilen ve yol test yüzeylerini temsil eden girişlerle yapılmıştır.

Anahtar Kelimeler: Çeyrek taşıt, elektro-mekanik, H_∞ kontrol, parametrik olmayan sistem tanımlama metodları, parametrik sistem tanımlama metodları

CHAPTER 1

INTRODUCTION

1.1 Literature Review

The study of vehicle dynamics and suspensions started in the early 1930s in order to manufacture comfortable vehicles suited to fast motor traffic. Then in the following years the ride comfort and handling trade-off problem is first recognized. This made the suspension problem, a problem of ride comfort, body motion, road handling and suspension displacement. Studies of semi-active suspensions started in 1950's. The idea of adding an active component was introduced later in the 1960's. In 1980's electronics and microprocessors began to be adopted in suspension technology and suspensions with active and semi-active elements began to be commercialized. [1]

Today, we implement various electronically controlled control systems in cars, such as active suspensions, antilock brake systems, cruise control, traction control, and four wheel steering. Antilock brake systems, traction control systems and cruise control system are equipped on many of production vehicles while active suspensions and four wheel steering are less common and still being studied. Control of vehicle dynamics became a popular subject in time and active suspensions are being studied since a long time. The road disturbance transmission problem in an active suspension is covered by the study of control systems. [2]

Today, by the development of electronics technology, cost of a control system gets cheaper day by day. As the control systems get more cost efficient, they may soon be ready to be installed in most of production vehicles. However active suspension systems also need a

high power supply. They are still expensive and difficult to implement for wide spread commercial use. Today they are used only in luxury vehicles.

The requirements of a good passenger comfort and road handling have become stricter than ever before in recent decades, making suspension systems rely more and more on the development of computer modeling and simulation methods.

In the industry, modelling of suspension systems and other mechanical systems are done with the help of computers. ADAMS/CAR and CarSim are some of the widely used computer modelling programs in suspension modeling. Corporate automobile companies also have their own software.

Various modeling methods for dynamic systems have been developed in the fields of mechanical and civil engineering. System identifiation techniques also have been used in a variety of pyhsical and economic processes. [9] Parametric system identification methods are used to identify a system with a mathematical structure model, it is identified by using algorithms and related parameters, whereas nonparametric methods model a system directly by its responses. The non-parametric identification methods for the system such as the impulse response characteristics and frequency response are also considered with a mechanical perspective in this work.

As the modeling is done, H_∞ control methods are practiced on the system. H_∞ methods were first given in 1981 and studied to this day. The original formulation of H_∞ is given by Zames *et al.* in 1981. The Riccati solution of the H_∞ control, which is used in this work, were later given by Doyle *et al.* in 1989 for the linear time-invariant case. To see the state of the subject these years, a detailed analysis of H_∞ design can be seen in the book written by Knobloch *et al*. in 1993. Some examples of PID, robust multivariable controllers and applications of optimal control theory that were developed these years can be seen in the literature (Thompson, 1976, 1989; Karnopp 1983; Majeed 1989; Ray 1991). Later, the linear matrix inequalities solution of the H_∞ control was given by Boyd *et al.* in 1994. There are researches done on H_∞ control problems with time domain constraints for single input single output (SISO) and multi input multi output (MIMO) systems (H. Rotstein and A. Sideris 1991-1995). A two degree of freedom loop shaping observer based H_∞ design discussed in

Skogestad and Postlethwaite (2005); this design is based on the works of Hoyle et al. (1991), McFarlane and Glover (1992), Limebeer et al. (1993), Walker (1996). The design was formulated to meet certain frequency-domain specifications which also include robustness criteria given by Zhou and Doyle in 1998. [9-14]

As for health problems, some researches were done in the US in 1960s. Low back pain was the number one threat to professional drivers of heavy vehicles. Studies showed that the low frequency vibration is dominant in a heavy vehicle and is a strong factor of fatigue and stress of drivers as they sit in any posture for a long time (Kelsey *et al*. 1975; Paddan *et al,* 1988). [15] [16]

To obtain the handling performance or riding comfort, the performance indicator can be written as related to the values of output performance variables, the body acceleration, suspension displacement or a combination of these [17]. As for this work, the performance output is taken being equal to body acceleration and the aim is to improve the riding comfort.

1.2 Objective of the Thesis

Suspension types and some control aspects are mentioned below.

1.2.1 Conventional Suspensions (Passive Suspensions)

A traditional passive suspension system contains only springs and dampers. Its parameters are chosen and adjusted with respect to vehicle weight and driving conditions. These attributes differ with every vehicle model. As the vehicle would be driven in a city or as it would be used for transportation of goods or any other loads, it requires a different suspension with different values. These parameters are adjusted with the purpose of achieving a certain level of compromise between road handling and comfort for a car model. Passive suspension characteristics are fixed at certain values and does not change while driving. There are also no active or semi-active elements in a passive suspension structure. [4]

Conventional passive suspension systems are widely used in vehicles today due to their simplicity, small volume, low cost and high reliability. However in recent decades desired comfort and road handling ability keeps increasing. Suspension systems have structural limits, because of that, a passive suspension system can hardly improve the two properties at the same time. Therefore, passive suspensions cannot give enough satisfactory results against suspension problems thus semi-active suspensions and active suspensions are continuously researched by researchers today.

Active and semi-active suspensions have sensors, control algorithms, active or semi-active elements as distinct from passive suspensions. Here a few things about semi-active are given suspensions before the thesis proceeds to active suspensions.

1.2.2 Semi-Active Suspensions

Semi-active suspensions have identical structure and motion equations to passive suspensions but unlike passive suspensions, they have semi-active elements such as semi-active dampers which have continuously variable characteristics. Magneto rheological dampers are installed in some vehicles with semi-active suspensions (Audi TT, Honda Acura MDX).

Damping force and energy dissipation changes as the characteristics change, thus the semi-active damper provides a control. The characteristics of the semi-active damper are controlled through a controller making it softer or stiffer. The controller gets inputs from sensors as the driving conditions change.

Semi-active suspension control methods were developed widely in the literature. In the literature there are skyhook and groundhook control methods and a hybrid of those, which are all being used in general. In the skyhook method, the damper is assumed to be connected to the sky and in groundhook method, to the ground (Figure 1.1). These three methods provide different controls and there are also some works which compares them [5].

Semi-active suspensions with semi-active dampers are being implemented on production vehicles today. Semi-active elements require low energy levels and are cheaper compared to active suspensions.

Suspension control studies are done mostly for semi-active suspensions in suspension control studies.

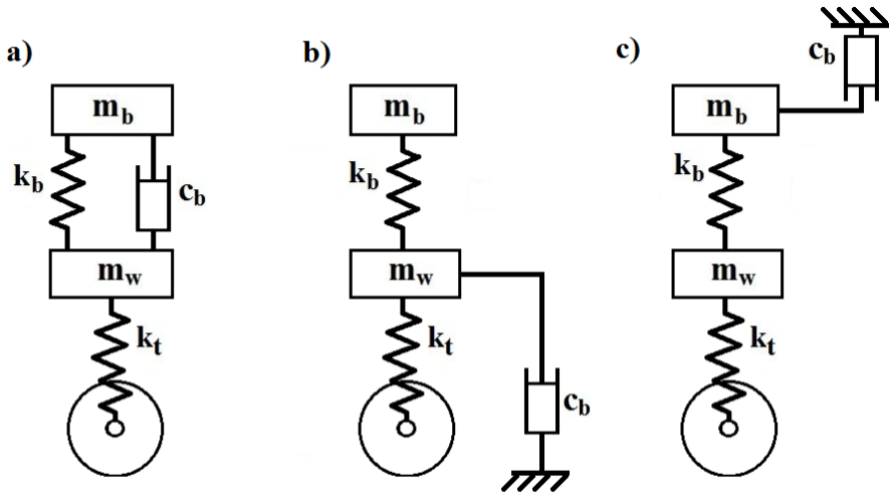

Figure 1.1 (a) Conventional suspension; (b) ground hook semi active suspension; (c) sky hook semi active suspension

1.2.3 Active Suspensions

There are various active suspension structures that are explained in the next section. In an active suspension, there is an extra force actuator included to the passive suspension structure that supplies an active force to the suspension. The active force is determined by the controller through signals. The controller has an algorithm generated and set beforehand to fit our aims. The controller design may be based on complex mathematical theories such as the control methods based on Hardy spaces, optimal control and robust control. Optimal and robust control methods are still studied for active suspensions. As the controller is being designed, required inputs are chosen to gather information from the system. In real life vehicle applications, the inputs are taken from sensors that were

attached to the parts of the vehicle and processed in the controller. Also in this work, a proper system output is chosen with respect to hardware structure.

1.2.4 Actuator Types of Active Suspensions

There are some types of actuators being used in active suspensions to provide the active force. These types are electromagnetic, pneumatic or hydraulic. Each has its own advantages and disadvantages and they are briefly explained below.

Hydraulic and pneumatic active suspensions — Hydraulic motors and hydraulic actuators are known for operating with high forces in the industry. They are widely used in heavy construction equipment however they are limited by acceleration and speed. On the other hand pneumatic motors and actuators are widely used in control applications and industry automation since they can quickly respond in starting and stopping times and operate in low forces.

Hydraulic and pneumatic active suspensions have a hydraulic or pneumatic actuator as the suspension actuator. This type of suspensions are mainly suited for low-bandwidth applications. Pneumatic and hydraulic actuators transmit the energy as the fluid pressures change. This pressure difference is created by a pump. This pump may be cam shaft driven which is rotated by the internal combustion engine or may be driven by an electric motor.

Active suspensions that are implemented in automobiles (Toyota Soarer) and racing cars (Lotus 99T) are mostly based on hydraulic or pneumatic operation or hydropneumatic operation (Opel Insignia, Citroën XM).

Electromagnetic active suspensions — An electromagnetic active suspension consists of an electric motor actuator which has an oil-free simple structure and provides better ride comfort and handling compared to other types of active suspensions. Control force is accurate and flexible. They have high-bandwidth operation, improved dynamic behavior and stability. The real system has two such electro-magnetic motors in the laboratory. [6]

1.3 Hypothesis

A suspension is a mechanical system of springs, dampers and other mechanical elements that connects a vehicle to its wheels. The system that is worked on in this thesis, is a custom made electro-mechanical system that represents an active suspension system. It is constructed to be used in The Scientific and Technological Research Council of Turkey (TÜBİTAK) project numbered 108E089 and entitled “Development and Optimal LPV control of an Active Suspension System Actuated by Linear Motors”. Initially an approach is made as the system is an ordinary mechanical system and some mechanical characteristics are thus evaluated, then the system is inspected as a suspension system.

The main function of a suspension is to isolate the vehicle body and its passengers from irregular road surfaces, cornering, acceleration, or deceleration. The car body motion (Figure 1.1) is examined as a combination of yaw, pitch, and roll motions. [7] Suspensions also carry the weight of the vehicle body.

Suspensions maintain a firm contact between the road and the tires, providing a handling. Automobile handling performance generally refers to how well a car responds to cornering and swerving. Suspensions play a crucial role in handling and riding comfort of a vehicle. Road handling and passenger comfort are examined as engineering problems in the literature. In control applications the main aim is to improve road handling abilities of a car and passengers’ comfort. [8] The thesis is focused on taking the comfort problem into consideration as an engineering problem.

There is a trade-off between the riding comfort and handling performance. Car body accelerations should be kept low for a better comfort. With soft springs, the car body have low car body accelerations but as a trade-off, the suspension mass have high values of displacement. This require a bigger rattle space but more importantly the handling performance gets worse. With stiffer springs, the suspension displacement is kept lower however, the transmission of the road disturbance gets higher. A damper with a low damping coefficient reduces the stability of a mechanical system. For a suspension system it would provide a more comfortable ride and improved vibration isolation but affect vehicle

reducing handling ability in an undesirable way since this causes high car body and suspension mass deflections. On the other hand a damper with a high damping coefficient provides a better handling and improved roll stability when cornering by effectively controlling the tires' road contact with small displacements. [3]

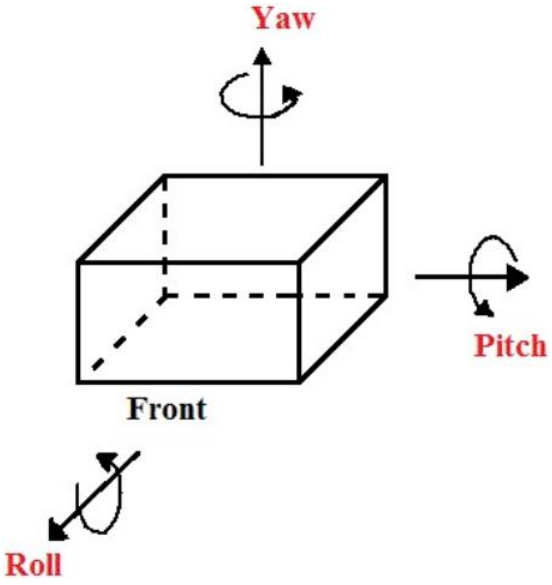

Figure 1.2 Car body motion

CHAPTER 2

MODELLING OF AN ACTIVE SUSPENSION SYSTEM

This section presents some models using the mechanical concepts, inertia, stiffness, damping elements and active force. These concepts determine the system's response to arbitrary inputs and helps us to determine how to modify the suspension characteristics to lighten the effects of the road.

2.1 Components and Characteristics of an Active Suspension

Brief explanations of the components of an active suspension system and the information that is used in latter sections are given here.

2.1.1 Linear Spring

A spring is an elastic mechanical link between two particals in a mechanical system. Spring steel is a low-alloy, medium-carbon steel or high-carbon steel with a very high yield strength. All springs are inherently nonlinear however the force and displacement are assumed to have a linear relationship according to Hooke's law [18]. This linear ratio is called the spring constant, *k*. Other elastic elements like steel rods are also treated like springs in machine dynamics studies.

Leaf springs, coil springs, torsion bar springs and air springs are widely used within vehicles. Air springs are rubber cylinders filled with compressed air that are being used in busses, trucks and trains. Leaf springs are nonlinear springs which appear in vehicle suspensions and they can even be seen in earliest car models. Helical coil springs basically have the same

laws with linear springs but have rotational displacement and axis. Springs grew to be more popular on passenger cars and trucks until today. [18]

The motion and energy equations of springs are stated below are going to be used in Lagrange and Newton mathematical modeling.

For a linear spring, let us say the unstretched lenght, without external forces is x_1 stretched lenght is x_2 and the spring deflection is $x_2 - x_1$. When the spring in compression, the deflection is negative. Springs are considered massless in mathematical equations and for calculations in this thesis.

Linear spring force-displacement law:

$$F = k(x_2(t) - x_1(t)) \tag{2.1}$$

Spring stores potential energy in compliance with a potential energy function. The equation that is used in the Lagrange equation is:

$$PE = \frac{1}{2}kx(t)^2 \tag{2.2}$$

The system (TÜBİTAK project number 108E089) contains 3 parallel springs as suspension spring component. Parallel springs of the system are shown below:

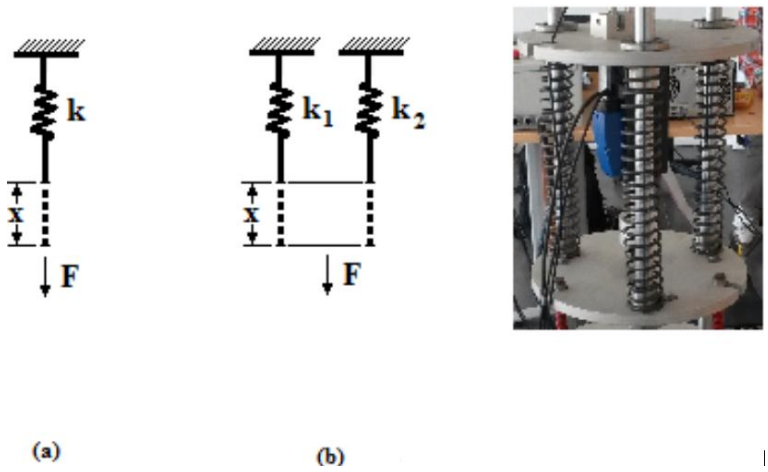

Figure 2.1 Parallel springs

When there are 2 springs parallel as shown in b (Figure 2.1), then their displacements are equal therefore the total force can be further mathematically expressed as such:

$$F = k_1 x(t) + k_2 x(t) = k_e x(t) \tag{2.3}$$

$$k_e = k_1 + k_2 \tag{2.4}$$

$$PE = PE_1 + PE_2 \tag{2.5}$$

$$PE = \frac{1}{2} k_1 x(t)^2 + \frac{1}{2} k_2 x(t)^2 = \frac{1}{2} (k_1 + k_2) x(t)^2 \tag{2.6}$$

Springs actually have non-linear elasticity, but all springs are taken as linear springs with respect to Hooke's law.

2.1.2 Viscous Damper

Dampers are cylinders filled with hydraulic oil or compressed gas.

As the suspension travels up and down the hydraulic fluid is forced by a piston through tiny holes, called orifices. The viscous fluid then flows in the cylinder. The damping force generated is proportional to the relative velocity between the two boundaries confining the fluid.

Damping controls the travel speed and resistance of the vehicle's suspension. An undamped car would oscillate up and down. Dampers create a dissipation effect that causes the response to decay over time for a system in free vibration. With proper damping levels, the car settles back to a normal state in a minimal amount of time. Using magneto rheological dampers, semi-active suspensions can be controlled by increasing or decreasing the resistance of the fluid flow in the damper. There are also other ways to control a semi-active suspension damper, however this is not delved in further.

Depending on the damper construction and the velocity range, the magnitude of the damper force is a nonlinear function of velocity and can also be approximated as a linear function of velocity.

Following are the motion and energy equations of dampers which are used in Newton and Lagrange equations.

c being the damping coefficient. Viscous damper force is:

$$F(\dot{x}) = c(\dot{x}_2(t) - \dot{x}_1(t)) \tag{2.7}$$

Viscous damper energy is:

$$E = c \int \dot{x}^2 \, dx \tag{2.8}$$

Rotational dampers have rotational displacement. The same equations also recognized for rotational dampers by using rotational coordinates. Dampers are also assumed massless in mathematical equations in this work.

2.1.3 Damping Ratio

When working on a suspension system, one must understand what the damping ratio is. The damping ratio is a parameter, usually denoted by ζ that characterizes the frequency response of a second order ordinary differential equation. This parameter is particularly important in the study of control theory. [18]

Between overdamped and underdamped cases there exists a critical damping case, in which the system's kinetic energy gets dissipated by the dissipation elements and frictions thus it stops without oscillating. In such a case the damping coefficient is called the critical damping coefficient.[18]

For a damped harmonic oscillator with mass *m*, damping coefficient *c*, critical damping coefficient c_c, and spring constant *k*, it can be defined as the ratio of the damping coefficient in the system's differential equation to the critical damping coefficient which is:[19]

$$\zeta = \frac{c}{c_c} \tag{2.9}$$

Where the system's equation of motion is:

$$m\ddot{x} + c\dot{x} + kx = 0 \tag{2.10}$$

and the corresponding critical damping coefficient is:

$$c_c = 2m\sqrt{\frac{k}{m}} \tag{2.11}$$

or

$$c_c = 2m\omega_n \tag{2.12}$$

where ω_n is called natural frequency which is described in the following part. It can be mentioned here as; as the damping effects get lower, the natural frequency of the system gets approximately equal to the resonance frequency.[19]

The damping ratio is a dimensionless value, being the ratio of two coefficients of identical units.

When ζ = 1, the system is said to be critically damped, in which the damping coefficient equals c_c. A critically damped system converges to zero as fast as possible without oscillating.

When ζ > 1, the system is over-damped and there are two different real roots. The damping coefficient c is larger than the critical damping co-efficient, c_c.

When 0 < ζ < 1, the system is under-damped. In this situation, the system oscillates at the natural damped frequency ω_d, which is a function of the natural frequency and the damping ratio. [20] [19]

When ζ=0 , the system is undamped; that is, the damping co-efficient c = 0. [19]

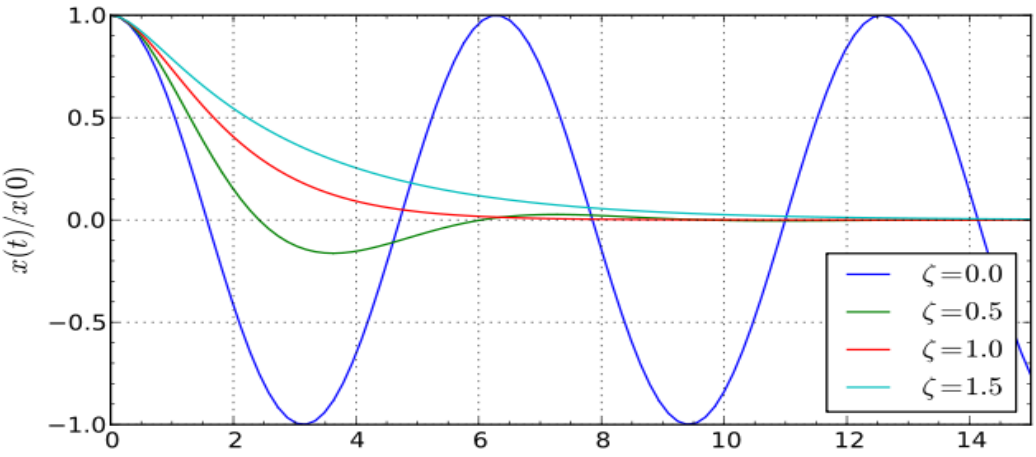

Figure 2.2 Damping ratio cases [21]

The system has two-degree of freedom on vertical axis. There should be two damping ratios taking the wheel damping in to account. From Newtonian equations if we put the differential equations of motion in a dimensionless form to find the damping ratios, we get:

$$\zeta_s = \frac{c_s}{\sqrt{m_s k_s}} \tag{2.13}$$

$$\zeta_u = \frac{m_s}{m_u}\frac{c_t}{c_s}\zeta_s \tag{2.14}$$

Damping ratio cases are as shown in Figure 2.2. However since tire dissipation (c_t) is ignored, there is only one damping ratio for the system [22].

2.1.4 Natural Frequency and Peak Frequency

Free vibration analysis of a mechanical system, resonance and peak frequency are important factors in frequency analysis studies and for the frequencies to be controlled.

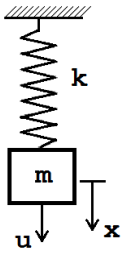

Figure 2.3: Free vibration

While describing the natural frequency with a simple undamped system, consider a completely reversible conservative system. The work done by the force is equal to the difference between the final and inital values of the potential energy function. The system is undamped and has a single degree of freedom, with a sine wave input that has the amplitude f_0 and the frequency ω_0 (Figure 2.3). [20] [19]

$$u = f_0 \sin \omega_0 \tag{2.15}$$

Applying Newton's second law of motion, the equation of motion is:

$$f_0 \sin \omega t = m\ddot{x} + kx \tag{2.16}$$

This is a brief explanation of detailed mathematical equations. Whose theories can be further read on in the mechanical vibrations book given by Schmitz *et al.* in 2012 [19]. There are homogeneous and particular solutions to this equation, x_h and x_p, being the former and latter respectively. The solution being:

$$x(t) = x_h(t) + x_p(t) \tag{2.17}$$

The homogeneous solution is:

$$x_h(t) = A_1 \cos \omega_n t + B_1 \sin \omega_n t \tag{2.18}$$

Where A_1 and B_1 are constants and ω_n is as:

$$\omega_n = \sqrt{\frac{k}{m}} \tag{2.19}$$

This is called natural frequency (undamped natural frequency). If we know an object's natural frequency, we have an idea on how it vibrates.

Free vibrations of any elastic body is called natural vibration and occurs at a frequency called natural frequency. All systems have a natural frequency, and many of systems have more than one. For instance quarter-car suspension systems have two natural frequency since they have two degrees of freedom. [23]

A linear, time-invariant system with a sine wave input at a steady state have a sine wave output of the same frequency as the input. But the amplitude and phase of the output is different from those of the input. The time difference between input and output is called phase shift and is also studied under frequency analysis.

The following is also a brief explanation of detailed mathematical calculations. The actual derivations of those equations are shown extensively and thoroughly in [24] and [25].

Phase angle φ, is the phase shift between the input sine wave and the output sine wave.

From motion equations and the phase angle;

$$\varphi = tan^{-1}\left(\frac{c\omega}{k - m\omega^2}\right) \tag{2.20}$$

The amplitude is:

$$x = \frac{f_0}{\sqrt{(k - m\omega^2)^2 + (c\omega)^2}} \tag{2.21}$$

In non-dimensional form it becomes:

$$\frac{xk}{f_0} = \frac{1}{\sqrt{\left[1-\left(\frac{\omega}{\omega_n}\right)^2\right]^2 + \left[2\zeta\left(\frac{\omega}{\omega_n}\right)\right]^2}} \tag{2.22}$$

$$tan\varphi = \frac{2\zeta\left(\frac{\omega}{\omega_n}\right)}{1-\left(\frac{\omega}{\omega_n}\right)^2} \tag{2.23}$$

[26]

Interpreting the following formulas:

$$\omega = 0 \rightarrow \varphi = 0° \tag{2.24}$$

$$\omega = \omega_n \rightarrow \varphi = -90° \tag{2.25}$$

$$\omega = \infty \rightarrow \varphi = -180° \tag{2.26}$$

Resonance ($\omega = \omega_n$):

In this case, the operation frequency matches the natural frequency. As $\frac{\omega}{\omega_n}$ goes to 1, $\left[1-\left(\frac{\omega}{\omega_n}\right)^2\right]$ goes to 0, making the frequencies overlap and make the system respond at a greater amplitude, which thus causes a big failure. However in real applications, considering friction and dissipation elements, infinite amplitudes are not expected but peak frequencies are. Peak frequencies become especially dangerous when there is small or no damping and friction. In peak frequencies, relevant states show high amplitudes, in this work they are the states that represent car body acceleration and suspension deflection. Passenger comfort and road handling are badly effected in those peak frequencies.

When designing machines, designers must calculate if the natural frequencies of the component parts matching driving vibrational frequencies of motors or other oscillating parts. [27]

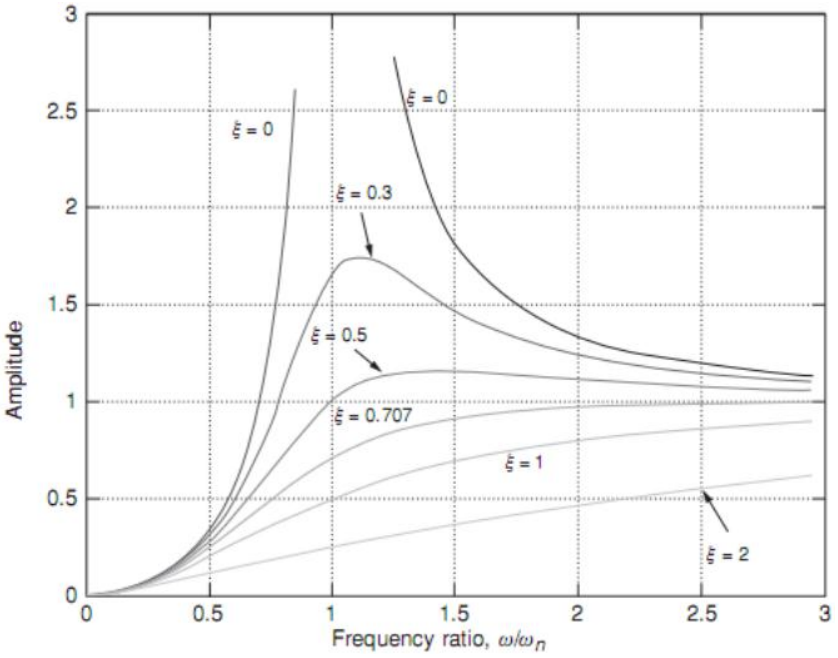

Figure 2.4 Amplitude peaks with various damping ratios.[27]

Amplitude peaks are as seen in Figure 2.4 for a single degree of freedom system. There are two natural frequencies for two degree of freedom systems. Consider a suspension system where tire stiffness is k_t , suspension spring constant k_s , sprung mass m_s and unsprungmass m_u. Natural frequencies are calculated by:

$$\omega_{n1} = \frac{1}{2}\left(\frac{k_s + k_t}{m_u} + \frac{k_s}{m_s}\right)\left(1 - \sqrt{1 - \frac{\frac{4k_s k_t}{m_s m_u}}{\left(\frac{k_t + k_s}{m_u} + \frac{k_t}{m_s}\right)^2}}\right) \tag{2.27}$$

$$\omega_{n2} = \frac{1}{2}\left(\frac{k_s + k_t}{m_u} + \frac{k_s}{m_s}\right)\left(1 + \sqrt{1 - \frac{\frac{4k_s k_t}{m_s m_u}}{\left(\frac{k_t + k_s}{m_u} + \frac{k_t}{m_s}\right)^2}}\right) \tag{2.28}$$

For a suspension system, amplitude peaks are expected to be as shown in this frequency-amplitude diagram, Figure 2.5. The points of the peak frequencies can be calculated by using formulas 2.27 and 2.28.

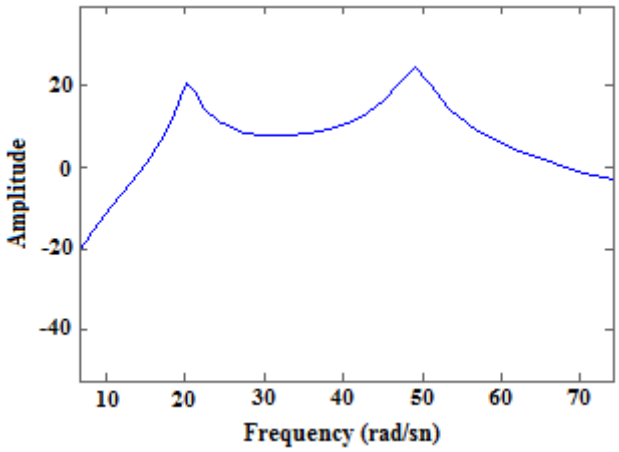

Figure 2.5 Amplitude peaks of a suspension

2.1.5 Transmissibility

Transmissibility is another subject that is important to understand machine dynamics and mechanical systems. It is defined as:

$$TR = \frac{Displacement\ of\ transmitted\ force\ or\ motion}{Displacement\ of\ exciting\ force\ or\ motion} \tag{2.29}$$

Transmissibility ratio is studied as force and displacement transmissibility. It gives us an idea of how much of the input force and motion are transmitted to the output. [28] It can be used in equations for minimizing or controlling the transmission of motion or disturbance force.

TR is calculated from motion equations, natural and operation frequencies. The formula for displacement transmissibility (TR_d) is:

$$TR_d = \frac{[1 + (2\zeta r)^2]^{\frac{1}{2}}}{[(1 - r^2)^2 + (2\zeta r)^2]^{\frac{1}{2}}} \tag{2.30}$$

$$r = \frac{\omega}{\omega_n} \tag{2.31}$$

Where *r* is the dimensionless frequency ratio of natural and operating frequencies. Force transmissibility (TR_f) is identical to displacement transmissibility and given by:

$$TR_f = TR_d r^2 \text{ [29]} \tag{2.32}$$

In case there is no dissipation force and $\zeta = 0$, the transmissibility ratio is 1 and *r* is equal to $\sqrt{2}$ .When $r = \sqrt{2}$ (and $TR_d = 1$), the transmitted force is equal to input force, for $r > \sqrt{2}$, $TR_d < 1$ the force transmissibility increases as the damping ratio increases and damping components work better. So for a good vibration isolation the system should be designed so that when $r > \sqrt{2}$, the damping constant *c* is as small as possible ($\zeta \approx 0$). For a suspension system, this means high suspension mass travel amplitudes and this reduces road handling ability. If *k* were to be low, the natural frequency would also be low so that *r* may easily be greater than $\sqrt{2}$. When *r* is smaller than $\sqrt{2}$, the frequency is getting closer to the resonance frequency (r=1). [27]

2.2 Mathematical Modeling

There are quarter car, half car and full car models used in the literature [30]. Each of those models have advantages over the others for different research purposes. For instance front half car models are used in rolling motion studies and side half car models are used in car pitching motion studies. Rolling motion and pitching motion are studied with car cornering, acceleration and breaking [30]. The load changes with the number of passengers and/or luggage; inertia forces change at the acceleration, braking and cornering times. Quarter car models are simpler, making it a better option in the study of control techniques.

Quarter vehicle model is based on dividing the vehicle in four parts which leads to four 2-DOF models. There are two masses in a quarter car model, vibration of body mass (m_b) and suspension mass (m_w). They are also named as sprung mass (body mass) and unsprung mass (suspension mass).

2.2.1 Traditional Passive Suspension Quarter Car Model

This is a well-known passive quarter-car model, a spring-mass-damper model. A linear spring with stiffness, *k* and a viscous damper with damping coefficient, *c* are connected in parallel to the inertia element, *m*. Also adding an external displacement, motion equations are obtained of this system (Figure 2.6) in the vertical direction. The motion equations of Figure 2.6 are written by Newton's second law of motion.

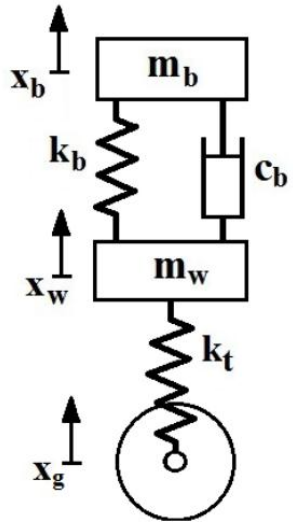

Figure 2.6: Traditional passive suspension quarter car model

The masses (m_b, m_w) move along the directions (x_b, x_u) and the force balances are written for these axis. The tyre between the axle and the road surface is treated as a spring and damper couple, but since the damping constant of the tyre is very small in value, it is negligible for the sake of convenience in the motion equations. Using the balance of forces, here we state spring and damper formulas for each mass.

Equations of motion for a passive suspension:

$$m_b\ddot{x}_b = -k_b(x_b - x_w) - c_b(\dot{x}_b - \dot{x}_w) \tag{2.32}$$

$$m_w\ddot{x}_w = k_b(x_b - x_w) + c_b(\dot{x}_b - \dot{x}_w) - k_t(x_w - x_g) \tag{2.33}$$

2.2.2 Active Suspension Quarter Car Models for Various Applications

Some active suspension types can be found throughout the literature. These suspension types can be seen being used for specific bandwidth applications. Schemes (Figure 2.7) and motion equations (2.34-2.40) of the indicated active suspension types are stated below.[17]

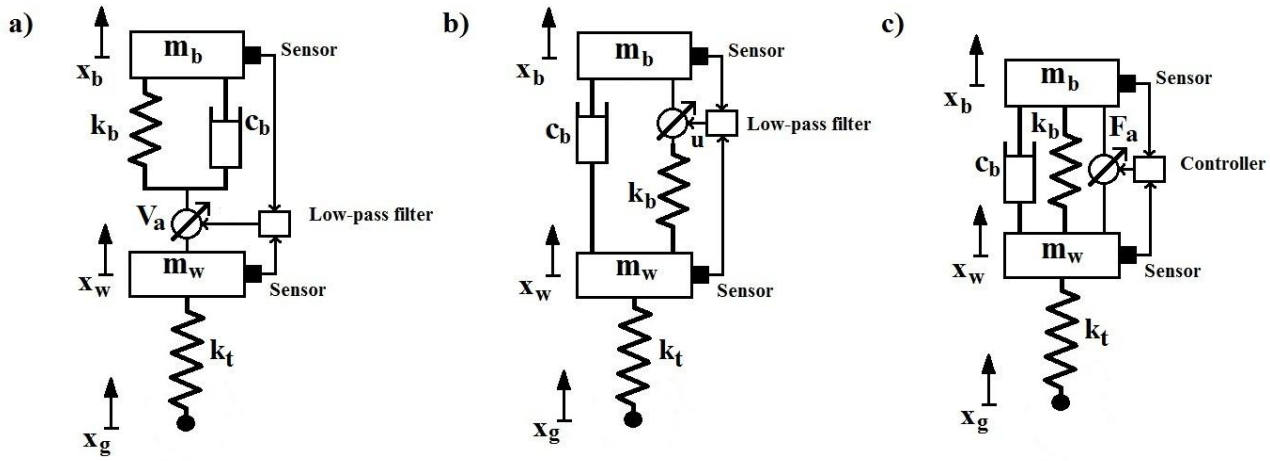

Figure 2.7 (a), (b) Low bandwidth type active suspension; (c) high bandwidth active suspension

In low bandwidth type suspensions, we can see applications where the actuator is placed in series with the spring or in series with the spring and the damper (Figure 2.7).

Motion equations of the models (Figure 2.7) are:

a)

$$V_a = \dot{x}_b - \dot{x}_w \tag{2.34}$$

$$m_b\ddot{x}_b = -k_b(x_b - x_w) - c_b(\dot{x}_b - \dot{x}_w) \tag{2.35}$$

$$m_w\ddot{x}_w = k_b(x_b - x_w) + c_b(\dot{x}_b - \dot{x}_w) - k_t(x_w - x_g) \text{ [31]} \tag{2.36}$$

b)

$$m_b\ddot{x}_b = -k_b(x_b - x_w) + k_b u - d_b(\dot{x}_b - \dot{x}_w) \tag{2.37}$$

$$m_w\ddot{x}_w = k_b(x_b - x_w) + c_b(\dot{x}_b - \dot{x}_w) - k_t(x_w - x_g)$$ [32] (2.38)

c)

$$m_b\ddot{x}_b = F_a - k_b(x_b - x_w) - c_b(\dot{x}_b - \dot{x}_w)$$ (2.39)

$$m_w\ddot{x}_w = -F_a + k_b(x_b - x_w) + c_b(\dot{x}_b - \dot{x}_w) - k_t(x_w - x_g)$$ [31] (2.40)

While a low bandwidth type suspension aims to control the suspension over the lower frequency range, and specifically around the rattle space frequency, the high bandwidth active suspension targets especially the higher frequency range.

CHAPTER 3

SYSTEM IDENTIFICATION TECHNIQUES

System identification techniques are being used for various types of systems like mechanical systems, thermodynamic systems and markets. By examining a dynamical system we may deduce its characteristics and gain a general idea about it, we can examine it's frequency characteristics and also can acquire a mathematical model by means of measured input and output data; these are within the system identification field. System identification is used as time series analysis. There are various algorithms, models and analysis methods used for various systems. Basic models and analysis methods are mentioned in this chapter. The system identification methods used in this work are based on Lennart Ljung methods. MATLAB system identification toolbox includes all common techniques of Lennart Ljung system identification techniques. [9] [33]

System identification techniques are mainly divided in two methods: non-parametric and parametric system identification.

3.1 Non-parametric System Identification Techniques

Non-parametric system identification methods are used to obtain a general idea about a system and to determine the frequency band of interest. A systems transient response and frequency behaviours are examined under non-parametric system identification.

No structure assumptions are made other than that the system being linear. Non-parametric system identification methods gather information about the transfer function with direct techniques. Time-domain non-parametric system identification methods are

response analysis and correlation analysis methods. Frequency domain non-parametric system identification methods are sine-wave testing, fourier analysis and spectral analysis.

It is practical to use non-parametric system identification methods before using parametric system identification methods, that helps us to evaluate parametric system identification methods. [9]

3.1.1 Transient Response Analysis

Transient response analysis involves very simple analysis methods such as impulse response analysis and step response analysis. Such analyses can be made for a given transfer function, with *impulse* and *step* functions as inputs under the system identification toolbox. Transient analyses have large error margins in most practical applications. However, correlation analysis may be used to determine basic control characteristics such as delay time, statistic gain and dominating time constants,. Some characteristic numbers can be graphically constructed by this way. [9]

3.1.2 Correlation Analysis

Correlation analysis is an impulse response analysis. MATLAB is able to help with this method by defining a Finite Impulse Response(FIR) model and making an estimation using least squares method. This analysis can be done by using the GUI, choosing the menu item Estimate>Correlation Model. Fequency domain information about the system can not be gained with this method as this is a transient response analysis.

3.1.3 Frequency analysis

Frequency analysis is a simple analysis to learn about the frequency response of a linear system. Frequency response is one of the basic properties of a system. By applying a sine wave input and measuring the system response, we can detect the amplitude and phase shift values of the signals. As explained previously in modelling section, there are two amplitude peaks we expect to see and the frequency response characteristics of the real system are used in order to make interpratations in the next chapter. And this information

may be vital for suspension systems regarding passenger health problems and frequency peaks. It is already explained that quarter car suspension models have two frequency peaks as they have two degree of freedoms. These two peak frequencies are examined in control applications. A frequency analysis test should be done for these frequencies of interest. The signals frequency spectrum also refers to its bandwidth.

3.1.4 Fourier Analysis and Spectral Analysis

These analyses are also in frequency domain. An empirical transfer function is estimated by taking the system as a linear system. We can use 'etfe' and 'fft' functions to estimate an empirical transfer function of the system in MATLAB. This approach is useful for highly resonant systems.

As fourier transformation applied to a time-domain signal, we find a representation of that signal in frequency domain. Fourier analysis is usually used with smoothing methods in literature [34]. This is done by presuming the values of the true transferfunction are related with eachother in different frequencies. Spectral analysis identifies the individual frequency components presented as amplitude and phase. We can use 'etfe' and 'spa' functions to estimate the frequency spectra of transfer functions. These functions give information about the input and output and frequency range.

3.2 Parametric System Identification Techniques

Parametric system identification methods are used to estimate the internal structure and parameters of a system. This is done by doing estimations by the input and the output data. In parametric system identification, there are various models that are used with various methods [9] [35]. Some of those methods and models are briefly explained in the next parts.

To begin the system identification procedure a model and a fit criterion are defined and the data is obtained by applying a suitable input signal and measuring the corresponding output. Then we obtain a set of candidate models using the measured data. The set of candidate models are validated to find the best corresponding model for our system. After obtaining

the candidate models, an appropriate parameterization is adjusted and validated for the selected structure. This way, the best corresponding values are determined.

Similar to dynamic models, system identification models also should not be accepted as "perfect" models. Instead it is said that a particular model may be enough to describe the characteristics of our system.

The models we found may not be good enough to represent our system, in such a case, the data gathering experiment, chosen model or fit criterion should be changed until an acceptable model is found.

The mentioned structures and methods are explained below along with the grey box-black box concept. But before that input signals of the data gathering experiment are explained.

3.2.1 Input Signals of the Data Gathering Experiment

A suitable input signal must be applied to the system in order to acquire the required data. There are some common input options for system identification. One such option is to apply a filtered white noise signal, which is generated from a combination of random numbers. This signal is filtered through a linear filter. It is a statistical noise that has Gaussian distribution. We can achieve a variety of signal spectrums by choosing a proper filter. This makes it a random signal with a constant power spectral density. [35]

Other options are; using a random binary noise or a pseudo-random binary noise, which has a sequence of binary numbers. Pseudo-random signal appears to be random; but in fact it consists of a repetitive sequence of pulses which makes it deterministic. There are also signals based on the sine wave, such as the chirp signal or a sine sum signal. Chirp signal is a sine wave signal whose frequency increases or decreases at a linear rate with time. It covers a wide band of frequency and may be used in early experiments.

Sine-sum input signal is the input signal that is being used in this work. The data is gathered with an identification experiment. The sine waves were created by a combination of random numbers. Random numbers determine and randomize the frequency and phase values of the sine waves and thus the input covers a frequency spectra. The sine sum signal

is periodic in principal, however it acts as a non-periodic signal in the experiments for the period time is greater than the experiment time.

3.2.2 Grey box- Black box

The models that are explained in this section might be reffered as black box models. As for grey box identificaiton, linear ordinary differential equations are used.

“Grey box model” term is used in the case of known internal structure and only when the parameters are estimated from input and output data. We can make a more accurate estimation with a grey box model since we know the structure.

“Black box model” term is used in the case of unknown motion equations and internal structure. We guess the order of the system when using a black box model. Systems are taken as black box models generally in the literature.

3.2.3 Model Structures

In system identification, LTI models are generally described with:

$$y(t) = G(q,\theta)u(t) + H(q,\theta)e(t) \tag{3.1}$$

Where $u(t)$ denotes the input and $e(t)$, the white noise disturbance. Some common special models in literature are ARX, ARMAX and state-space structures. ARX is a basic model which the input and output terms are written separately. Similarly to (3.1) we can describe the ARX model with:

$$y(t) = \frac{B(q)}{A(q)}u(t) + \frac{1}{A(q)}e(t) \tag{3.2}$$

AR, ARMAX, Output-Error and Box-Jenkins models are based on the basic ARX model. Selecting a model is important since a different model may result in distinct solutions. Mathematical representations of the remarked models are briefly stated below. A,B,C,D,F being the shift operators, they are presented as follows:

$$A(q) = 1 + a_1 q^{-1} + \cdots + a_{n_a} q^{-n_a} \tag{3.3}$$

$$B(q) = b_1 + b_2 q^{-1} + \cdots + b_{n_b} q^{-n_b+1} \tag{3.4}$$

$$C(q) = 1 + c_1 q^{-1} + \cdots + c_{n_c} q^{-n_c} \tag{3.5}$$

$$D(q) = 1 + d_1 q^{-1} + \cdots + d_{n_d} q^{-n_d} \tag{3.6}$$

$$F(q) = 1 + f_1 q^{-1} + \cdots + f_{n_f} q^{-n_f} \tag{3.7}$$

ARX model structure is:

$$\begin{aligned} y(t) + a_1 y(t-1) + \cdots + a_{n_a} y(t-n_a) \\ = b_1 u(t-n_k) + \cdots + b_{n_b} u(t-n_k-n_b+1) + e(t) \end{aligned} \tag{3.8}$$

In a simple representation:

$$A(q)y(t) = B(q)u(t) + e(t) \tag{3.9}$$

ARX relates the current output (y) to a finite number of past outputs $y(t-k)$ and inputs $u(t-k)$. n_k is taken equal to 1 if there is no dead-time, n_a is taken equal to the number of poles and $n_b - 1$ equal to the number of zeros of the system.

ARMAX model structure:

$$\begin{aligned} y(t) + a_1 y(t-1) + \cdots + a_{n_a} y(t-n_a) \\ = b_1 u(t-n_k) + \cdots + b_{n_b} u(t-n_k-n_b+1) + c_1 e(t-1) + \cdots \\ + c_{n_c} e(t-n_c) + e(t) \end{aligned} \tag{3.10}$$

This can be represented in a simple form as:

$$A(q)y(t) = B(q)u(t-n_k) + C(q)e(t) \tag{3.11}$$

Output-Error Model is as written:

$$y(t) = \frac{b_1 u(t-n_k) + \cdots + b_{n_b} u(t-n_k-n_b+1)}{u(t-n_k) + f_1 u(t-n_k) + \cdots + f_{n_1} u(t-n_k-n_b)} + e(t) \tag{3.12}$$

It is written in a simple representation as:

$$y(t) = \left[\frac{B(q)}{F(q)}\right] u(t-n_k) + e(t) \tag{3.13}$$

Box-Jenkins Model is as shown:

$$y(t) = \left[\frac{B(q)}{F(q)}\right] u(t-n_k) + \left[\frac{C(q)}{D(q)}\right] e(t) \tag{3.14}$$

And the well known State Space model is :

$$\frac{dx(t)}{dt} = A\, x(t) + B\, u(t) + K\, e(t) \tag{3.15}$$

$$y(t) = C\, x(t) + D\, u(t) \tag{3.16}$$

The indicated models are used with computer based iterations in MATLAB, system identification toolbox. It requires experience to easily determine which model and method should be chosen.

3.2.4 Identification Methods

The estimation is done by evaluating the candidate models (candidate parameters) with mathematical methods. Mathematical evaluation methods are briefly explained below.

Prediction error minimization method — This method is based on iterative minimization of a criterion. In prediction error method, the prediction error is evaluated by being filtered through a stable linear filter.

A model structure, a filter as the predictor and a scalar function as the criterion are initially chosen in this technique. The prediction error is described as the difference between output and the predicted output. It is evaluated by being filtered through a stable linear filter. Using this filter, the effects of high frequency disturbances, non-essential terms like slow drift terms and similar values can be removed. A scalar valued function is used to assess the performance of the predictor. Calculating a scalar valued function, the avarage of the error is found in the time interval $1 \leq t \leq N$. Thus V_N is found. $V_N(\theta, Z^N)$ is a natural measure of the validity model $M(\theta)$. V_N is then minimized by calculating '$\arg\min V_N(\theta, Z^N)$' and estimated parameters are calculated.

Least-Square Methods for Linear Regression method — In this method, prediction error method is used for all time intervals $1 \leq t \leq N$ and squares of the errors are summed and minimized.

The least square method is the standart approach to estimate unknown systems and is used in wide range of engineering calculations. In system identification studies, using the ARX structure, the criterion function $V_N(\theta, Z^N)$ is written by taking the filter, $L(q) = 1$ and the scalar function, $l = \frac{1}{2}\varepsilon^2$. This way the sum of squares is minimized.

N4SID method — N4SID is not an iterative method. There are no difference between zero and non-zero initial states in the N4SID method. This method is especially useful for high order multi variable systems. In MATLAB, N4SID method uses a separate linear least-square step to re-estimate the B, D matrices and the initial state. [36] [9]

Instrumental variable method — This method is widely used in economics. In this methods the instruments that effects the system are examined. It is based on describing the weak and strong instruments that form the system. This method can be used with "ivar", "ivx" "iv4", functions.

CHAPTER 4

EXPERIMENTAL TEST SYSTEM

4.1 Description of the Experimental System

The system that is used in this work has been previously developed in a TÜBİTAK project (project number 108E089). It can be seen in Figure 4.1. It is a mechanical system that contains two sets of three springs, two linear motors, masses and an electrical panel.

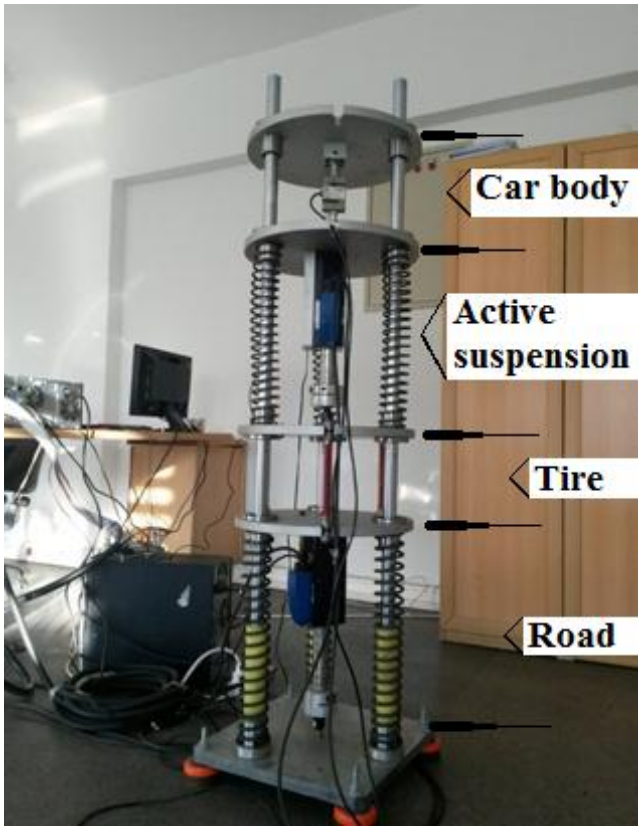

Figure 4.1: The system in the laboratory

4.1.1 System contents and their functions

The system can be tought as two parts as upper and lower. While the upper mass represents the car body, the middle mass represents the suspension mass.

For the lower half, there are three springs and a magnetic motor. The road displacement was simulated by this part of the system. It has the capability of simulating any kind o road conditions that occurs in the real world. This generated road surface is the disturbance input to the active suspension system which is the upper half of the spring-damper-mass system.

The upper part consists of 3 other springs, the upper motor and a mass that represent the car body. The upper 3 parallel springs represent suspension springs.

The system doesn't have any dissipation elements installed however there are many friction forces on the rods and other elements. Since the friction energy is proportional with the velocity of the masses we may consider such frictions as damper dissipations in the mathematical equations. There are some mathematical models that include/exclude the dissipation effects in the next parts.

The system has the software and hardware equipment required to acquire the analog data and convert it to a digital signal. The upper-motor displacement data is taken as system output. There is an acceleration sensor attached to the upper mass. It's data is taken as the performance output. This signal is then presented in the MATLAB workspace.

Motors — The motors are linear servotube actuators. They have electromagnetic motor characteristics; they have high bandwidth operation and their force is stable and flexible. Electromagnetic motors have a simple structure, they are quiet and it is easy to work with them. They also have magnetic bearings which makes them perfectly linear and built in position sensors to gather the position data. They are attached to masses and their rods extend down to the other mass. The sensors measure the displacament of the masses by measuring the displacement of the rod in them as the motors are driven by the electrical panel.

The motor modal is SERVOTUBE Copley Controls, XTB38 with serial winding. They have a continuous force varying between 137 N to 276 N and 744 N to 1860 N peak force, 244 m/s^2 peak acceleration and they operate up to 6.2 m/s velocity without payload.

Initially some mathematical models are constructed by using the physical laws of the above mentioned elements and then they are evaluated with some non-parametric system identification methods. There are some nonlinearities and uncertainties in every real life mechanical system. It is important to remember that the examined system also has some.

4.2 Mathematical Modeling of the Experimental Setup

In this part the system is modeled with the help of Lagrangian energy equations and Newton's second law of motion. Prior knowledge of a spring-damper-mass system is already given in the second chapter.

Figure 4.2 is a drawn figure of our active suspension system in our university laboratory. The mathematical equations are stated with the expressions in Figure 4.2.

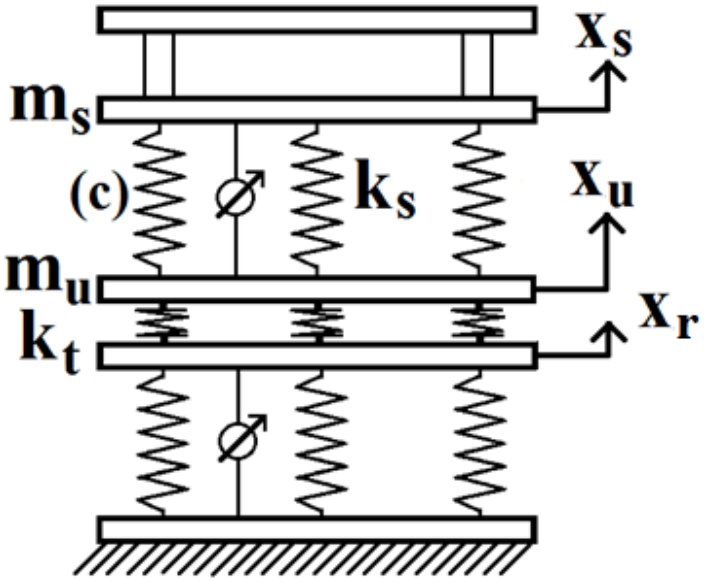

Figure 4.2: Drawn scheme and states of the system

It is impossible to reflect any mechanical system perfectly accurate to a real life application. Instead engineers should provide the best fitting model or a model close enough to the real system for the intended applications.

Road handling performance and the suspension deflection are inversely proportional. Upper motor displacement data ($x_s - x_u$) gives the displacement difference between the car body and suspension mass. This data is utilized and used to understand the active suspension's road handling ability.

The lower displacement data gives the road displacement, x_r. This road displacement is created by the lower motor and springs with respect to a chosen disturbance function.

High accelerations are known to effect the passenger comfort in a bad way. Car body acceleration is a parameter that helps us to understand the passenger comfort performance. Its reasoning includes the human bone structure and its position under certain forces that occurs with acceleration. The sprung mass represents the car body and its acceleration data ($\ddot{x}_s$) can be considered as comfort performance factor.

There is an output vector that represents the systems performance output. This vector can be written as being equal to $\ddot{x}_s$ for passenger comfort, ($x_s - x_u$) for road handling or as a weighted sum of the two for the mutual case. It is up to the engineering problem which should be selected. Once the model is decided, a controller then may be designed for the selected performance criteria.

Initially, Lagrange method is used to derive the mathematical model. It is based on the balance between kinetic, potential and dissipation energies. This balance results in an equation for each axis. Relevant states and variables can be seen on the inspected axis in Figure 4.2. After the Lagrange equations are written for the moving masses. The state space representations are obtained by putting them together.

The system is also modelled by using Newton equations, to ensure. Newton's second law states that the acceleration of an object is directly proportional to the net force acting upon object and inversely proportional to the mass of it. The acceleration of a known mass can be found by summing spring, damper and other passive or active forces in a mechanical

structure. Newton's second law of motion may be written for translational motion, rotational motion or a combination of those two.

Explanations of the energy equations and the characteristics of the internal elements of an active suspension is previously given throughout Chapter 2. They are used in the general Lagrange energy equation:

$$\frac{\partial}{\partial t}\left(\frac{\partial KE}{\partial \dot{\theta}_i}\right) - \frac{\partial KE}{\partial \theta_i} + \frac{\partial PE}{\partial \theta_i} + \frac{\partial DE}{\partial \dot{\theta}_i} = 0 \qquad i = 1,2 \tag{4.1}$$

Where KE, PE and DE denote kinetic energy, potential energy and damping energy respectively and $\theta_1 \triangleq x_s, \theta_2 \triangleq x_u$.

In order to improve the fitting performance of the model with respect to real ouput data, this thesis proposes a procedure. Proposed procedure initialy finds a model of the passive system by omitting the damper forces as there are no dampers in the real system.

In a sequel, the kinetic energy of the system is given by:

$$KE = \frac{1}{2} m_s \dot{x}_s{}^2 + \frac{1}{2} m_u \dot{x}_u{}^2 \tag{4.2}$$

The potential energy of the system is written as:

$$PE = \frac{1}{2} k_s (x_s - x_u)^2 + \frac{1}{2} k_t (x_u - x_r)^2 \tag{4.3}$$

Applying the straight forward calculations in Lagrange equations as follows:

$$\frac{\partial KE}{\partial \dot{x}_s} = m_s \dot{x}_S \tag{4.4}$$

$$\frac{\partial}{\partial t}\left(\frac{\partial KE}{\partial \dot{x}_s}\right) = m_s \ddot{x}_s \tag{4.5}$$

$$\frac{\partial PE}{\partial x_s} = -x_u k_s + x_s k_s \tag{4.6}$$

Similarly:

$$\frac{\partial KE}{\partial \dot{x}_u} = m_u \dot{x}_u \tag{4.7}$$

$$\frac{\partial}{\partial t}\left(\frac{\partial KE}{\partial \dot{x}_u}\right) = m_u \ddot{x}_u \tag{4.8}$$

$$\frac{\partial PE}{\partial x_u} = k_t x_u + k_s x_u - k_s x_s - k_t x_r \tag{4.9}$$

$$\ddot{x}_s(m_s) + x_u(-k_s) + x_s(k_s) = 0 \tag{4.10}$$

$$\ddot{x}_u(m_u) + x_r(-k_t) + x_u(k_s + k_t) + x_s(-k_s) = 0 \tag{4.11}$$

If the states are chosen as, $x_s, x_u, \dot{x}_s, \dot{x}_u$, the performance output is taken as $z = \ddot{x}_s$, and the system output as $y = x_s - x_u$, the fourth-order state space representation of the system becomes:

$$\begin{bmatrix} \dot{x}_s \\ \dot{x}_u \\ \ddot{x}_s \\ \ddot{x}_u \end{bmatrix} = \begin{bmatrix} 0 & 0 & 1 & 0 \\ 0 & 0 & 0 & 1 \\ \frac{-k_s}{m_s} & \frac{k_s}{m_s} & 0 & 0 \\ \frac{k_s}{m_u} & \frac{-k_s - k_t}{m_u} & 0 & 0 \end{bmatrix} \begin{bmatrix} x_s \\ x_u \\ \dot{x}_s \\ \dot{x}_u \end{bmatrix} + \begin{bmatrix} 0 \\ 0 \\ 0 \\ \frac{k_t}{m_u} \end{bmatrix} x_r \tag{4.12}$$

$$y = \begin{bmatrix} 1 & -1 & 0 & 0 \end{bmatrix} \begin{bmatrix} x_s \\ x_u \\ \dot{x}_s \\ \dot{x}_u \end{bmatrix}, \; z = \begin{bmatrix} \frac{-k_s}{m_s} & \frac{k_s}{m_s} & 0 & 0 \end{bmatrix} \begin{bmatrix} x_s \\ x_u \\ \dot{x}_s \\ \dot{x}_u \end{bmatrix} \tag{4.13}$$

According to the procedure, damping effects are included in the model. Even though there are no dampers in the real system, friction dissipations are modeled as damper dissipations:

$$\frac{\partial DE}{\partial \dot{x}_u} = c(\dot{x}_u - \dot{x}_s)\,, \frac{\partial DE}{\partial \dot{x}_s} = c(\dot{x}_s - \dot{x}_u) \tag{4.14}$$

The Lagrange equations can be formed as:

$$\ddot{x}_s(m_s) + \dot{x}_s(c) + \dot{x}_u(-c) + x_u(-k_s) + x_s(k_s) = 0 \tag{4.15}$$

$$\ddot{x}_u(m_u) + \dot{x}_u(c) + \dot{x}_s(-c) + x_r(-k_t) + x_u(k_s + k_t) + x_s(-k_s) = 0 \tag{4.16}$$

The state space representation of the second model with dissipation energies is written with the same system and performance outputs:

$$\begin{bmatrix} \dot{x}_s \\ \dot{x}_u \\ \ddot{x}_s \\ \ddot{x}_u \end{bmatrix} = \begin{bmatrix} 0 & 0 & 1 & 0 \\ 0 & 0 & 0 & 1 \\ \frac{-k_s}{m_s} & \frac{k_s}{m_s} & \frac{-c}{m_s} & \frac{c}{m_s} \\ \frac{k_s}{m_u} & \frac{-k_s - k_t}{m_u} & \frac{c}{m_u} & \frac{-c}{m_u} \end{bmatrix} \begin{bmatrix} x_s \\ x_u \\ \dot{x}_s \\ \dot{x}_u \end{bmatrix} + \begin{bmatrix} 0 \\ 0 \\ 0 \\ \frac{k_t}{m_u} \end{bmatrix} x_r \tag{4.17}$$

$$y = \begin{bmatrix} 1 & -1 & 0 & 0 \end{bmatrix} \begin{bmatrix} x_s \\ x_u \\ \dot{x}_s \\ \dot{x}_u \end{bmatrix} \quad z = \begin{bmatrix} \frac{-k_s}{m_s} & \frac{k_s}{m_s} & \frac{-c}{m_s} & \frac{c}{m_s} \end{bmatrix} \begin{bmatrix} x_s \\ x_u \\ \dot{x}_s \\ \dot{x}_u \end{bmatrix} \tag{4.18}$$

At this point the active force energy is added to the system and the model of the active system is found.

The new KE with the active force is:

$$KE = \frac{1}{2} m_s \dot{x}_s{}^2 + \frac{1}{2} m_u \dot{x}_u{}^2 + F(x_s - x_u) \tag{4.19}$$

$$\frac{\partial KE}{\partial x_s} = F \tag{4.20}$$

$$\frac{\partial KE}{\partial x_u} = -F \tag{4.21}$$

Motion equations are formed as given:

$$\ddot{x}_s(m_s) + \dot{x}_s(c) + \dot{x}_u(-c) + x_u(-k_s) + x_s(k_s) - F = 0 \tag{4.22}$$

$$\ddot{x}_u(m_u) + \dot{x}_u(c) + \dot{x}_s(-c) + x_r(-k_t) + x_u(k_s + k_t) + x_s(-k_s) + F = 0 \tag{4.23}$$

The state space representation of the active model is:

$$\begin{bmatrix} \dot{x}_s \\ \dot{x}_u \\ \ddot{x}_s \\ \ddot{x}_u \end{bmatrix} = \begin{bmatrix} 0 & 0 & 1 & 0 \\ 0 & 0 & 0 & 1 \\ \frac{-k_s}{m_s} & \frac{k_s}{m_s} & \frac{-c}{m_s} & \frac{c}{m_s} \\ \frac{k_s}{m_u} & \frac{-k_s - k_t}{m_u} & \frac{c}{m_u} & \frac{-c}{m_u} \end{bmatrix} \begin{bmatrix} x_s \\ x_u \\ \dot{x}_s \\ \dot{x}_u \end{bmatrix} + \begin{bmatrix} 0 & 0 \\ 0 & 0 \\ 0 & \frac{1}{m_s} \\ \frac{k_t}{m_u} & \frac{-1}{m_u} \end{bmatrix} \begin{bmatrix} x_r \\ F \end{bmatrix} \tag{4.24}$$

$$y = [1 \quad -1 \quad 0 \quad 0] \begin{bmatrix} x_s \\ x_u \\ \dot{x}_s \\ \dot{x}_u \end{bmatrix}, \; z = \begin{bmatrix} \frac{-k_s}{m_s} & \frac{k_s}{m_s} & \frac{-c}{m_s} & \frac{c}{m_s} \end{bmatrix} \begin{bmatrix} x_s \\ x_u \\ \dot{x}_s \\ \dot{x}_u \end{bmatrix} + [0 \quad 1] \begin{bmatrix} x_r \\ F \end{bmatrix} \tag{4.25}$$

An active system model is given in the last representation by omitting the damping effects.

$$\ddot{x}_s(m_s) + x_u(-k_s) + x_s(k_s) - F = 0 \tag{4.26}$$

$$\ddot{x}_u(m_u) + x_r(-k_t) + x_u(k_s + k_t) + x_s(-k_s) + F = 0 \tag{4.27}$$

$$\begin{bmatrix} \dot{x}_s \\ \dot{x}_u \\ \ddot{x}_s \\ \ddot{x}_u \end{bmatrix} = \begin{bmatrix} 0 & 0 & 1 & 0 \\ 0 & 0 & 0 & 1 \\ \frac{-k_s}{m_s} & \frac{k_s}{m_s} & 0 & 0 \\ \frac{k_s}{m_u} & \frac{-k_s - k_t}{m_u} & 0 & 0 \end{bmatrix} \begin{bmatrix} x_s \\ x_u \\ \dot{x}_s \\ \dot{x}_u \end{bmatrix} + \begin{bmatrix} 0 & 0 \\ 0 & 0 \\ 0 & \frac{1}{m_s} \\ \frac{k_t}{m_u} & \frac{-1}{m_u} \end{bmatrix} \begin{bmatrix} x_r \\ F \end{bmatrix} \tag{4.28}$$

$$y = \begin{bmatrix} 1 & -1 & 0 & 0 \end{bmatrix} \begin{bmatrix} x_s \\ x_u \\ \dot{x}_s \\ \dot{x}_u \end{bmatrix},\ z = \begin{bmatrix} \frac{-k_s}{m_s} & \frac{k_s}{m_s} & 0 & 0 \end{bmatrix} \begin{bmatrix} x_s \\ x_u \\ \dot{x}_s \\ \dot{x}_u \end{bmatrix} + \begin{bmatrix} 0 & 1 \end{bmatrix} \begin{bmatrix} x_r \\ F \end{bmatrix} \tag{4.29}$$

According to the procedure, the models are compared with the real system by outputs and it is seen that the best fitting model is the one that includes the dissipations effects. Therefore, the active model that includes the dissipation effects is used for control applications.

The same mathematical equations and state space representations can be found by using Newton equations. The Newton equations of the internal elements are also given through chapter 2. Therefore here only one of the stated models is briefly recalculated. The model that has damping effects and active force is calculated again directly from the following equations:

$$\ddot{x}_s m_s = -F_k - F_c + F \tag{4.30}$$

$$\ddot{x}_s m_s = k_s(x_s - x_u) - c(\dot{x}_s - \dot{x}_u) + F \tag{4.31}$$

$$\ddot{x}_u m_u = F_k - F_c + F_{k_t} - F \tag{4.32}$$

$$\ddot{x}_u m_u = k_s(x_u - x_s) - c(\dot{x}_u - \dot{x}_s) - k_t(x_u - x_r) - F \tag{4.33}$$

$$\ddot{x}_s(m_s) = \dot{x}_s(-c) + \dot{x}_u(c) + x_s(-k_s) + x_u(k_s) - F \tag{4.34}$$

$$\ddot{x}_u(m_u) = \dot{x}_s(c) + \dot{x}_u(-c) + x_s(k_s) + x_u(-k_s - k_t) + x_r(k_t) + F \tag{4.35}$$

As the equations are put together, the state space representation is:

$$\begin{bmatrix}\dot{x}_s\\ \dot{x}_u\\ \ddot{x}_s\\ \ddot{x}_u\end{bmatrix}=\begin{bmatrix}0 & 0 & 1 & 0\\ 0 & 0 & 0 & 1\\ \frac{-k_s}{m_s} & \frac{k_s}{m_s} & \frac{-c}{m_s} & \frac{c}{m_s}\\ \frac{k_s}{m_u} & \frac{-k_s-k_t}{m_u} & \frac{c}{m_u} & \frac{-c}{m_u}\end{bmatrix}\begin{bmatrix}x_s\\ x_u\\ \dot{x}_s\\ \dot{x}_u\end{bmatrix}+\begin{bmatrix}0 & 0\\ 0 & 0\\ 0 & \frac{1}{m_s}\\ \frac{k_t}{m_u} & \frac{-1}{m_u}\end{bmatrix}\begin{bmatrix}x_r\\ F\end{bmatrix} \tag{4.36}$$

$$y=\begin{bmatrix}1 & -1 & 0 & 0\end{bmatrix}\begin{bmatrix}x_s\\ x_u\\ \dot{x}_s\\ \dot{x}_u\end{bmatrix},\ z=\begin{bmatrix}\frac{-k_s}{m_s} & \frac{k_s}{m_s} & \frac{-c}{m_s} & \frac{c}{m_s}\end{bmatrix}\begin{bmatrix}x_s\\ x_u\\ \dot{x}_s\\ \dot{x}_u\end{bmatrix}+\begin{bmatrix}0 & 1\end{bmatrix}\begin{bmatrix}x_r\\ F\end{bmatrix} \tag{4.37}$$

Alternative performance output equations that are mentioned in part 4.2 are given as ($\ddot{x}_s$, (x_s-x_u) and $\ddot{x}_s+(x_s-x_u)$ respectively):

$$z=\begin{bmatrix}\frac{-k_s}{m_s} & \frac{k_s}{m_s} & \frac{-c}{m_s} & \frac{c}{m_s}\end{bmatrix}\begin{bmatrix}x_s\\ x_u\\ \dot{x}_s\\ \dot{x}_u\end{bmatrix}+\begin{bmatrix}0 & 1\end{bmatrix}\begin{bmatrix}x_r\\ F\end{bmatrix} \tag{4.38}$$

$$z_2=\begin{bmatrix}1 & -1 & 0 & 0\end{bmatrix}\begin{bmatrix}x_s\\ x_u\\ \dot{x}_s\\ \dot{x}_u\end{bmatrix}\quad,\quad (y=z_2) \tag{4.39}$$

$$z_T=\begin{bmatrix}\frac{-k_s+m_s}{m_s} & \frac{k_s-m_s}{m_s} & 0 & 0\end{bmatrix}\begin{bmatrix}x_s\\ x_u\\ \dot{x}_s\\ \dot{x}_u\end{bmatrix} \tag{4.40}$$

4.3 Non-parametric System Identification Approach

For the next step, known parameters are filled in the numeric model is acquired (see Appendix-a). A simulation is run with the mathematical model and from the results, it is seen that the numeric model are not consistent with the real system (Figure 4.3-4.4).

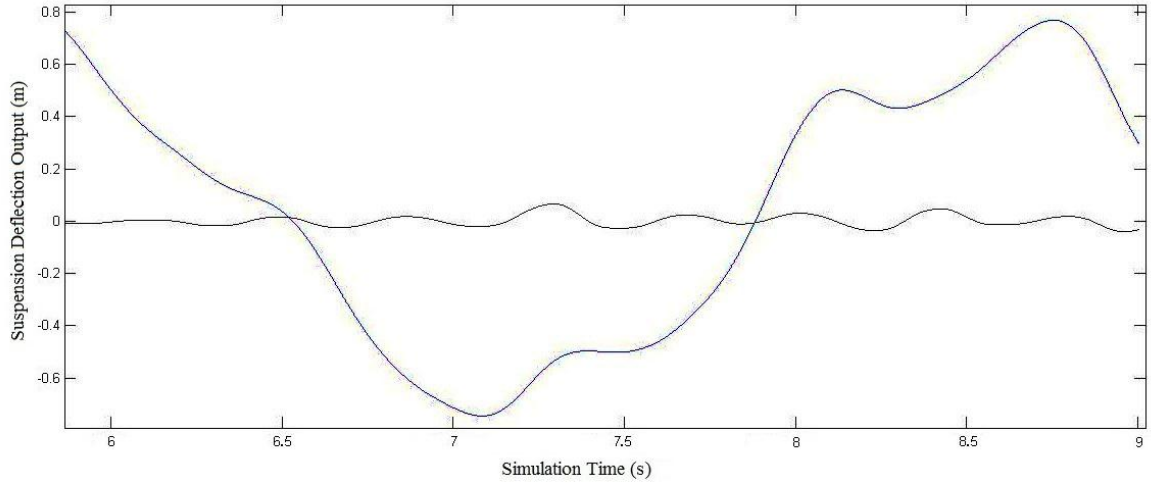

Figure 4.3 Suspension deflection output comparison (blue – mathematical model output, black – real system data)

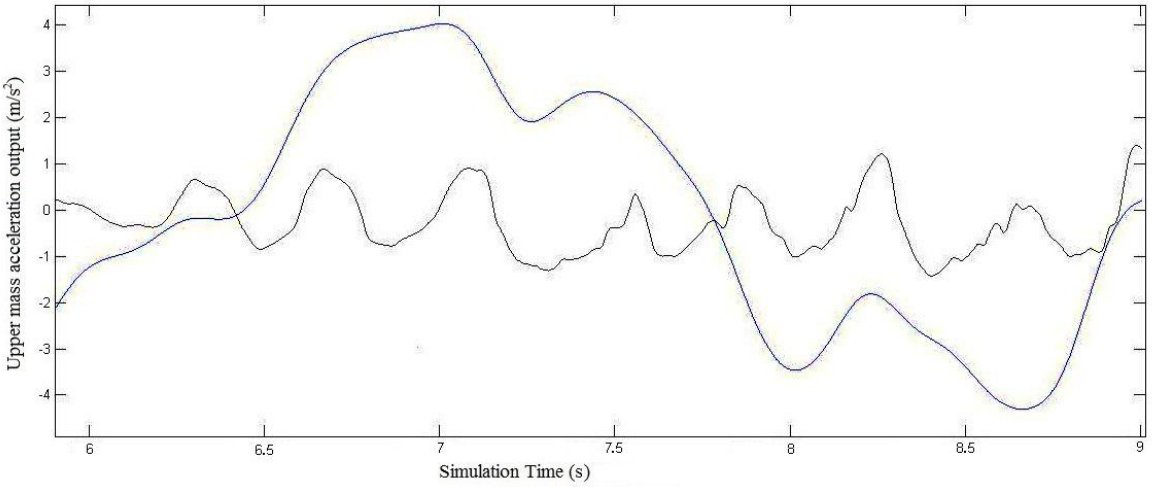

Figure 4.4 Upper mass acceleration output comparison of the mathematical model (blue – mathematical model output, black – real system data)

It is clear that the previously known mechanical parametes are wrong. However for we have the real system, we may include some basic non-parametric methods at this point in order to acquire a better mechanical model. The parameters of the system are evaluated and tuned around certain values and a tuned mathematical model is found. Frequency characteristics are examined through this part. With the help of previously explained concepts, frequency response and transient response characteristics are inspected in the following parts.

4.3.1 Transient Response Analysis

For the data gathering of the transient response analysis, the system is taken as a passive one and only the road input is applied to the system. From here, the real system should not be taken as any mechanical system instead, as a suspension system. To understand suspension spesific charateristics, the road input to upper mass displacment output should be taken into consideration.

If the experiment is repeated by using only the upper motor input, that would create an earthquake-effect on the system and force the system to show third degree of freedom characteristics.

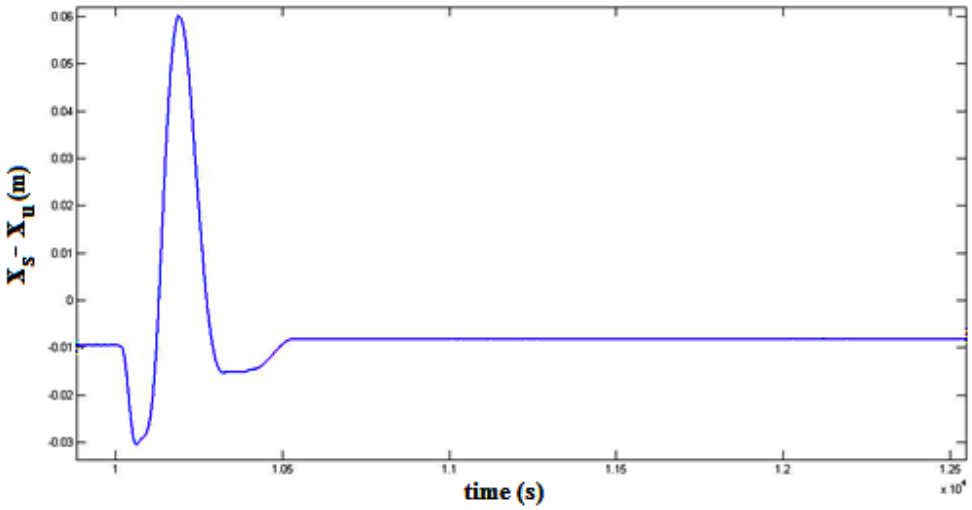

Figure 4.5 Transient response

To see the transient response, a shortened unit step input is applied as the road disturbance input. The response of the system is as shown in Figure 4.5. It is an underdamped response. From previously explained mechanics, it is seen that the damping ratio is between 0 and 1, much closer to 1.

4.3.2 Sine Wave Tests and Frequency Analysis

The input is taken as road disturbance and the output as upper mass deflection to see the tranmissibility properties. The lower motor applies the sine waves as road displacement inputs while x_s values are measured by the related displacement sensors. The experiment

is repeated five times for every fourty-eight frequency value in the Table 4.1. Different inputs with various frequencies are applied to note the different transmissibility ratios on a range of frequency. The ratio is the ratio of $\|x_s\|$ and $\|x_r\|$

The expression, $\|-\|$ represents the 2-norm (Euclidian norm). The average norm values are calculated from five values for every frequency value. The experiments take nine seconds each.

It is well known that higher frequencies than 100 rad/s do not result in high amplitude increase ratios in suspensions. Suspensions are always inspected between frequencies around 5-100 rad/s. This is due to the time constant the system. Also in this work, the experiments are limited around 3-85 rad/s.

By interpreting the results of the experiments, one can deduce the location of φ values which are around $-90°$.

Table 4. 1 Sine test results

Frequency (rad/s)	Ratio	Frequency	Ratio	Frequency	Ratio
3	1.3240	19	1.0703	37	0.3526
4	1.2881	20	0.9816	39	0.2969
5	1.2450	21	0.7546	41	0.2968
6	1.1850	22	0.7079	43	0.2456
7	1.0733	23	0.6164	45	0.2166
8	1.0387	24	0.5828	47	0.2356
9	1.0632	25	0.5444	49	0.1734
10	1.0026	26	0.4845	53	0.1598
11	1.0046	27	0.4289	57	0.1718
12	1.0214	28	0.4082	61	0.2102
13	1.0508	29	0.4651	65	0.2237
14	1.0953	30	0.4143	69	0.2594
15	1.1238	31	0.3831	73	0.2912
16	1.1905	32	0.3944	75	0.3135
17	1.1002	33	0.3990	77	0.3066
18	1.2282	35	0.3261	81	0.3202

Linear graph of the table is shown in Figure 4.6.

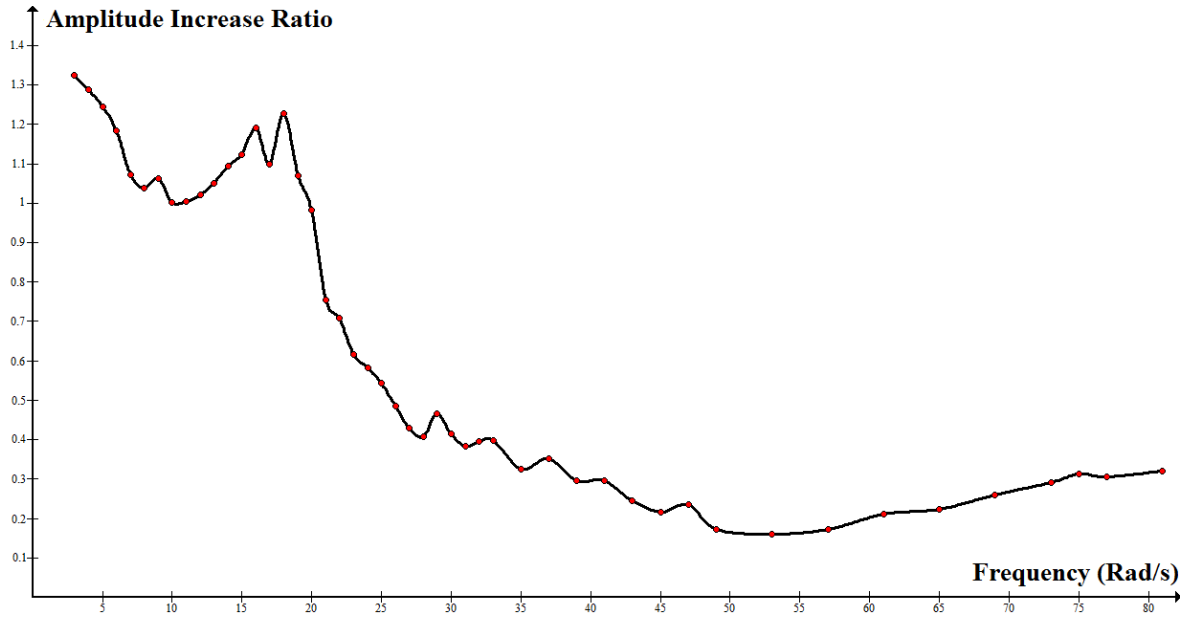

Figure 4.6 Drawn graph of the sine test results

The peak frequency locations are seen on lower frequencies. An H_∞ controller may be designed to reduce the outputs especially around these frequencies.

At this point, we can use this information to tune our mathematical model. There are some concepts that were explained in Chapter 2 that clarify the explanations of the analyses results. The information that are given in Chapter 2 states that the mass and spring constant values have a direct relationship with the location of the peak frequencies on the frequency band, which can be seen from the frequency test results. It is also stated that the dissipation constant value has a direct relationship with the rise of the Bode diagram. As the Bode diagram takes shape with accordence to these concepts, we may make a heuristic approximation by taking the labeled values as a base in order to achieve a better system output. The constant values are adjusted around certain values and a tuned model is acquired by this way. With the tuned model, more fitting system outputs are acquired and shown in Figure 4.8-4.9. The system outputs are compared with the real system outputs in the mentioned figures.

Tuned values are determined as: $m_S = 20$ kg, $m_u = 10$ kg, $k_S = 100$ N/m, $k_t = 100\ N/m$, $c = 20$ Ns/m

The following figure (Figure 4.7) is the Bode diagram of the tuned mathematical model that includes dissipation effects (see Appendix-b). The diagram is drawn on linear frequency axis (x_r input to x_s output) with absolute magnitude to make an easy comparison.

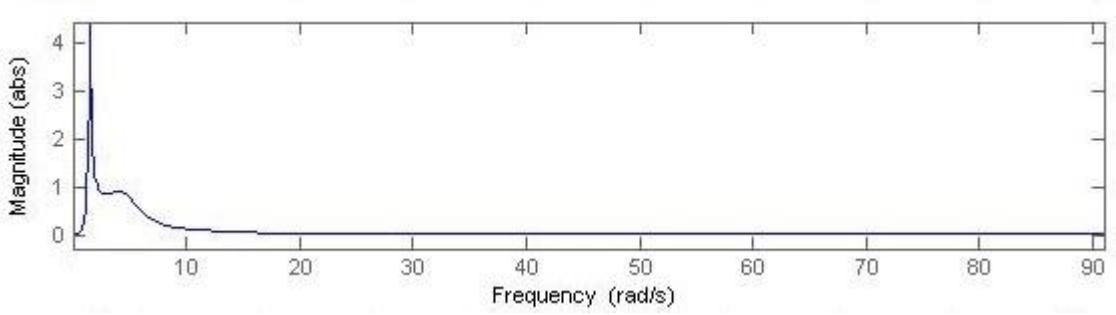

Figure 4.7 Bode diagram of the tuned mathematical model that includes the dissipation effects

The tuned mathematical model is given in a transfer function structure as follows:

Transfer function of the road disturbance input and the suspension deflection $(x_s - x_u)$ output:

$$TF_{11} = \frac{s^3 + 50s^2}{s^4 + 0.3s^3 + 25s^2 + s + 50} \tag{4.46}$$

Transfer function of the active force input and the suspension deflection $(x_s - x_u)$ output:

$$TF_{21} = \frac{-0.015s^3 - 0.75s^2 - 0.5s - 2.5}{s^4 + 0.3s^3 + 25s^2 + s + 50} \tag{4.47}$$

Transfer function of the road disturbance input and the sprung mass acceleration $(\ddot{x}_s)$ output:

$$TF_{12} = \frac{-10s^2}{s^4 + 0.3s^3 + 25s^2 + s + 50} \tag{4.48}$$

Transfer function of the active force input and the sprung mass acceleration $(\ddot{x}_s)$ output:

$$TF_{22} = \frac{0.15s^2 + 0.5}{s^4 + 0.3s^3 + 25s^2 + s + 50} \tag{4.49}$$

The suspension deflection output is as given in Figure 4.8. Evaluating the comparisons, Figure 4.3 with Figure 4.8 and Figure 4.4 with Figure 4.9, it is seen that the tuned model is much more consistent with the real system compared to the previous mathematical model.

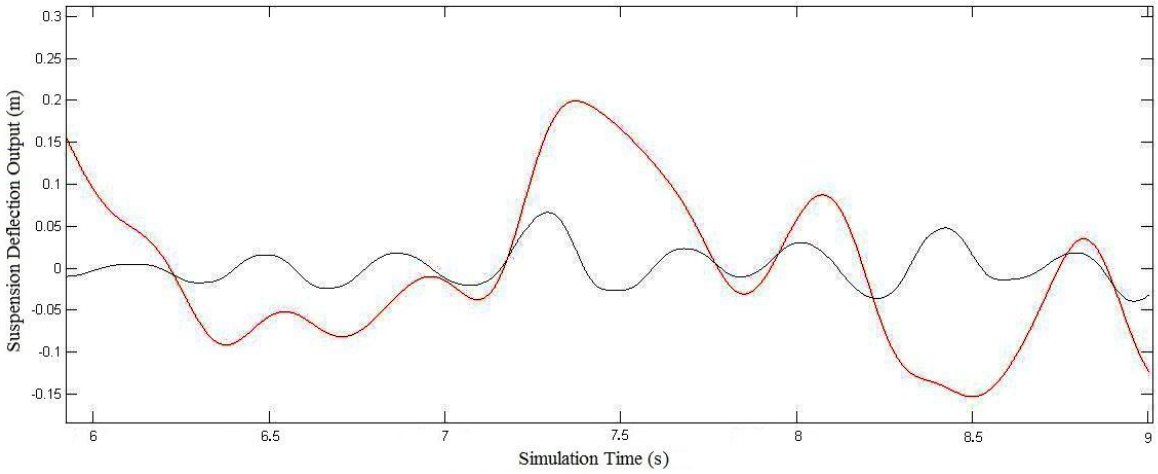

Figure 4.8 Suspension deflection output comparison (red – tuned mathematical model, black – real system data)

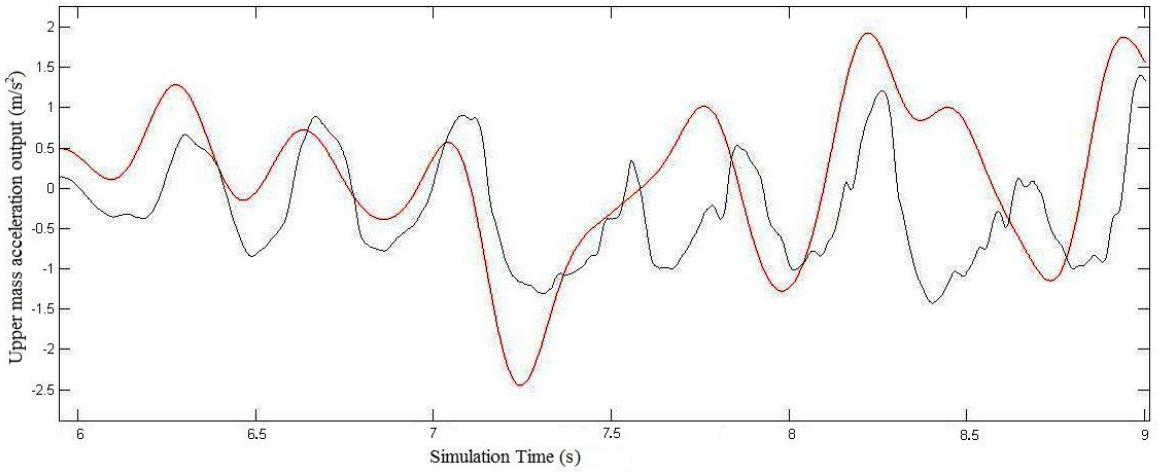

Figure 4.9 Upper mass acceleration output comparison (red – tuned mathematical model, black – real system data)

An accurate model is needed to get a good performance from the designed controller and other possible control applications. These analyses show that the mathematical models may not be good enough to represent the system and from this point the parametric system identification methods are included.

4.4 Parametric Approach

The internal structure of the real system is unknown. However, in this part it is treated as it is an unknown black box system. The system structure and parameters are deduced with respect to input and output data by comparing the candidate models.

A data gathering experiment is done to acquire the input and output data. The inputs are x_r and u (road disturbance and upper motor input respectively, Figure 4.10). The outputs, z and y (upper mass acceleration sensor and suspension deflection respectively) are measured by the sensors.

Figure 4.10 Black box

As already explained through chapter 3, we need input and output data for the system identification algorithm calculations. A wide range of frequency spectrum is included in the calculations by choosing proper inputs.

According to the general system identification procedure, initially an experiment is conducted to gather the required data for the parametric system identification techniques. The inputs are chosen as sums of sine signals and are applied by each of the two motors (Figure 4.11).

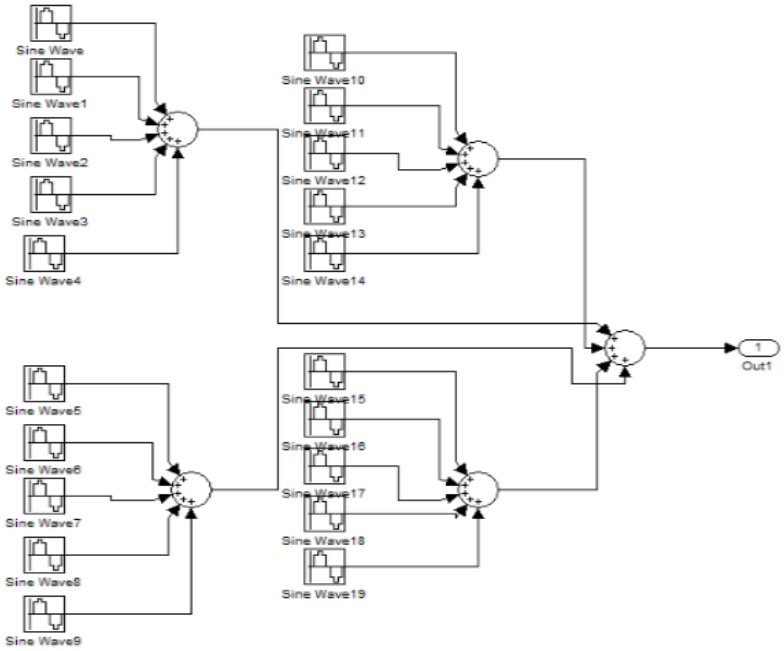

Figure 4.11 Sine sum input scheme

N4S4 model —A state space model is designed with the N4SID method (see Appendix-c). State space structure is taken as fourth order. Real output data and y and z outputs of the N4S4 simulations are as seen in Figure 4.12-4-13 respectively. Average errors are 0.00547 for the y output and 0.243 for the z output. [37]

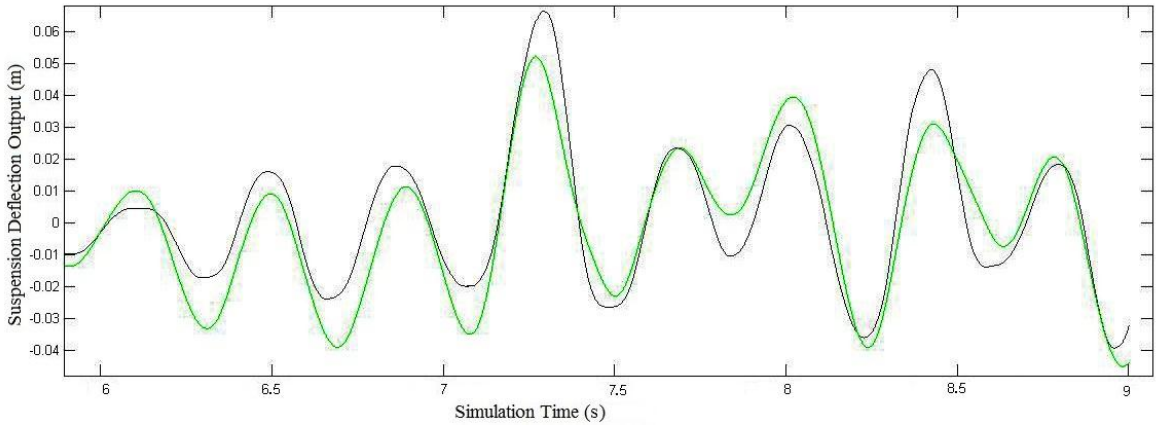

Figure 4.12 Suspension deflection output comparison (green – N4S4 model, black – real system)

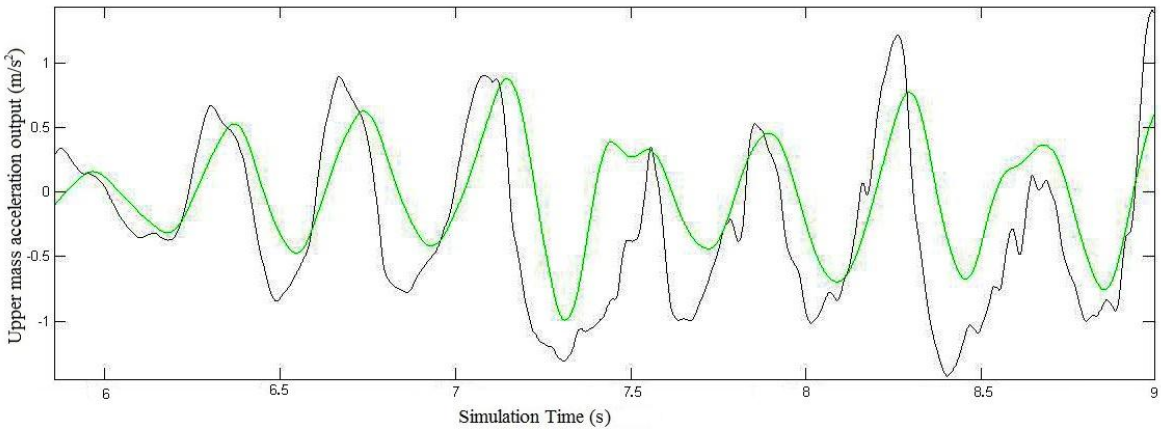

Figure 4.13 Upper mass acceleration output comparison (green – N4S4 model, black – real system)

Mathematical, tuned mathematical and N4S4 models output are compared below in a single graph for each output (Figure 4.14-4.15).

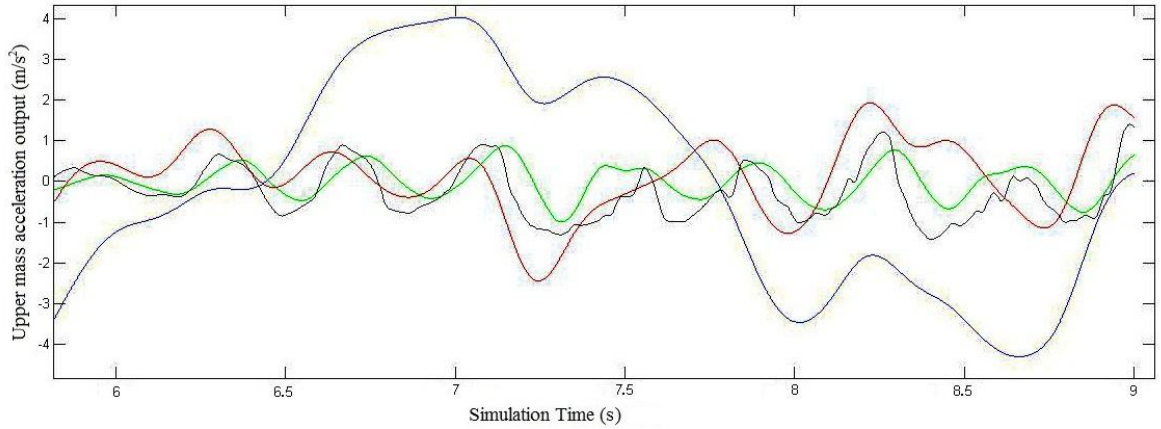

Figure 4.14 Upper mass acceleration output comparison (blue – mathematical model, red – tuned mathematical model, green – N4S4 model, black – real system data)

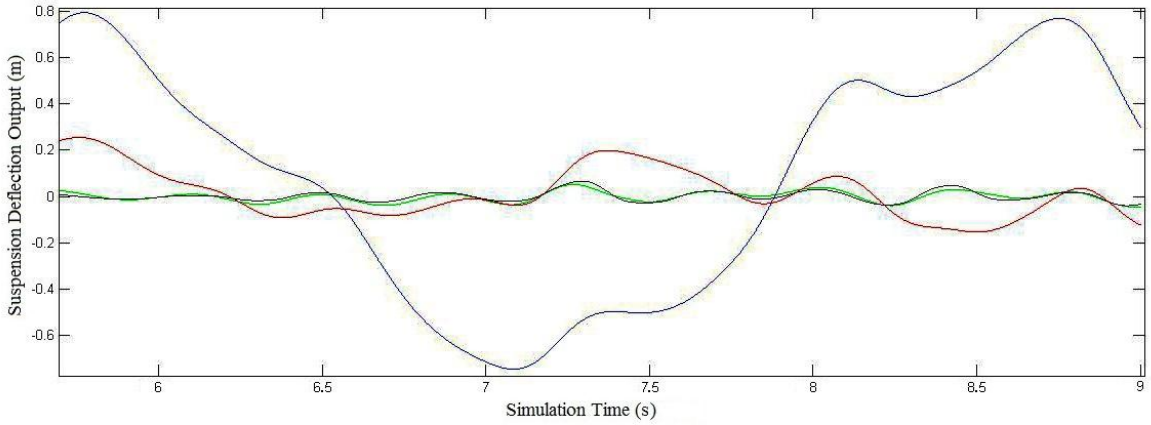

Figure 4.15 Suspension deflection output comparison (blue – mathematical model, red – tuned mathematical model, green – N4S4 model, black – real system data)

Average errors are founded by calculating the absolute values:

Table 4.2 Average errors of the models

Model	Upper mass acceleration avarage error	Suspension deflection avarage error
Mathematical	1.611	0.29725
Tuned mathematical	0.84	0.11271
N4S4	0.243	0.00547

The simulation scheme that is used in the simulations of this chapter is as shown in Figure 4.16.

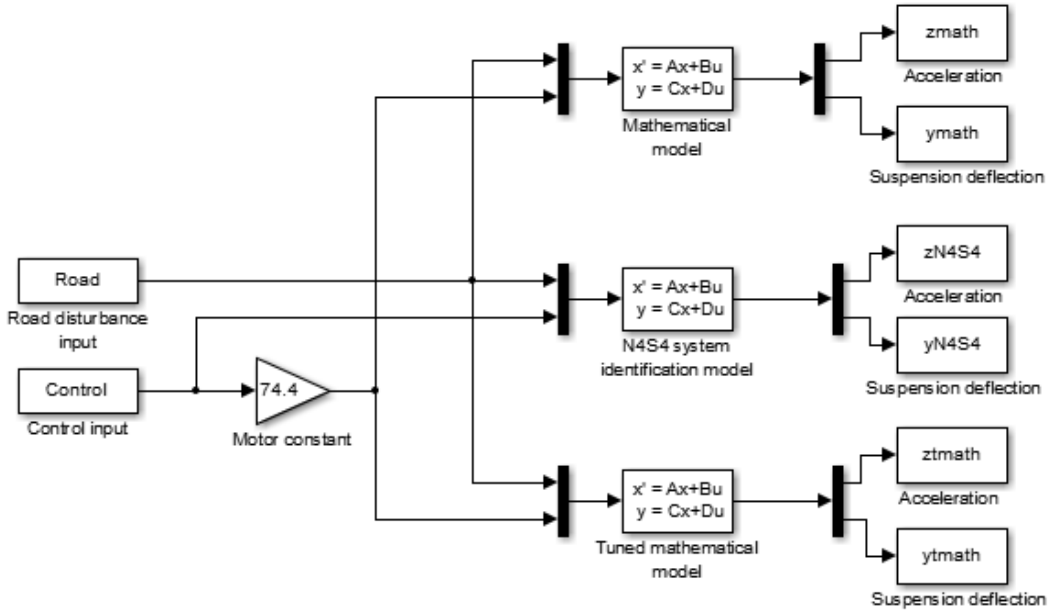

Figure 4.16 Simulation scheme

CHAPTER 5

MULTI INPUT-MULTI OUTPUT FEEDBACK CONTROL OF THE SYSTEM

In this chapter, output feedback control is the chosen control method which is used by taking the system output as the control output. The system outputs of the models are previously determined through Chapter 4.

The main problem is examined as passenger comfort in this chapter. As mentioned before, passenger comfort is related with the car body acceleration. Hence the upper mass acceleration is taken as the performance output. The proposed control mechanism aims to minimize the infinity norm of the transfer function between the disturbance signal(input) and performance signal(output performance). By using the feedback control, the effects and transmission of the road disturbance to the performance output are thus reduced.

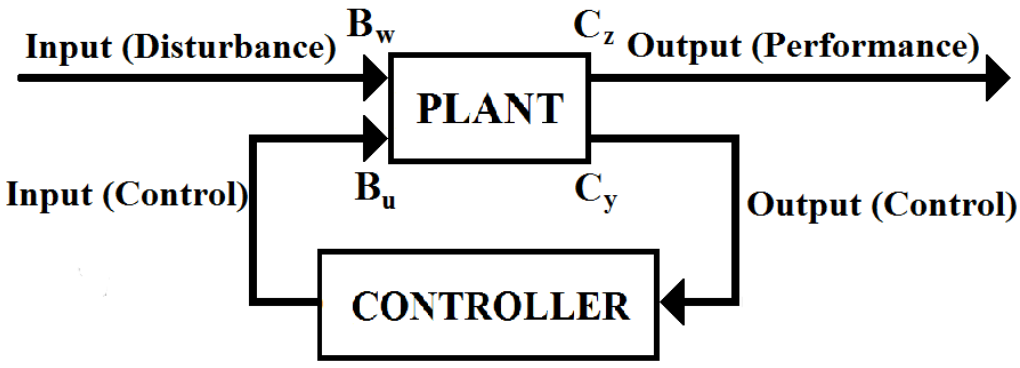

Figure 5.1 MIMO feedback scheme

The design of the MIMO feedback control system is as shown in Figure 5.1. The process of a feedback control system has three crucial phases. These are the measuring phase, the

filtering phase and the feedback phase. Initially the control output signals are measured and sent to the controller. Then the signal is fedback to the plant after proccessing the measurement in the controller. Thus, a control on the system is made possible. [38] In the real system the input B_w is the mechanical input created by the lower motor and lower three springs and the signal B_u is fed to the upper motor.

Realistically we may not have perfect description of an actual system. Plant models must be found that represents the system These models reflect the real systems physical properties and when defining a system model there are some limitations that should be considered, such as variability and operating conditions. Various models of the real system are already presented in Chapter 4 and these models are used as plants in this chapter. As some controllers are designed, this chapter is concluded by comparing and examining the results of the closed loop systems.

Let us consider a state space model as the plant and a state space structured controller. To indicate the system matrices and to find the dynamic feedback control equations for the combined structure of a feedback MIMO system [40]. The traditional state-space system structure is:

$$\dot{x} = Ax + Bu \tag{5.1}$$

$$y = Cx + Du \tag{5.2}$$

where $x \in \mathbb{R}^n$ denotes states of the system. Take the dynamic feedback controller as:

$$\dot{x}_C = A_C x_C + B_C y \tag{5.3}$$

$$u = C_C x_C + D_C y \tag{5.4}$$

The system is a MIMO system and has two inputs. Therefore the input matrix may be represented as:

$$B = [B_w \quad B_u]\,, \tag{5.5}$$

Here, B_u is the control input matrix and B_w is the disturbance input matrix as also shown in Figure 5.1. In a similar manner, the output matrix is:

$$C = [C_z;\ C_y] \tag{5.5}$$

$$D = \begin{bmatrix} D_{zw} & D_{zu} \\ D_{yw} & D_{yu} \end{bmatrix} \tag{5.6}$$

Here, $\mathrm{C_z}, \mathrm{D_z}$ and $\mathrm{C_y}, \mathrm{D_y}$ represents the performance outputs and the control outputs respectively. In regard to the mathematical model and system identification models, they are related with car body acceleration and suspension deflection.

$$u = C_c x_c + D_c y = C_c x_c + D_c C x + D_c D_{yw} w \tag{5.7}$$

$$y = C_y x + D_{yw} w \tag{5.8}$$

$$\begin{aligned} z &= C_z x + D_{zw} w + D_{zu} u \\ &= \left(C_z + D_{zu} D_c C_y\right) x + D_{zu} C_c x_c + (D_{zw} + D_{zu} D_c D_{yw}) w \end{aligned} \tag{5.9}$$

$$\dot{x} = Ax + B_w w + B_u u = \left(A + B_u D_c C_y\right) x + B_u C_c x_c = (B_w + B_u D_c D_{yw}) w \tag{5.10}$$

In matris form;

$$\begin{bmatrix} \dot{x} \\ \dot{x}_c \\ z \end{bmatrix} = \begin{bmatrix} A + B_u D_c C_y & B_u C_c & B_w + B_u D_c D_{yw} \\ B_c C_y & A_c & B_c D_{yw} \\ C_z + D_{zu} D_c C_y & D_{zu} C_c & D_{zw} + D_{zu} D_c D_{yw} \end{bmatrix} \begin{bmatrix} x \\ x_c \\ w \end{bmatrix} \tag{5.11}$$

$$x_{cl} = \begin{bmatrix} x \\ x_c \end{bmatrix} \tag{5.12}$$

And the closed-loop system is,

$$\dot{x}_{cl} = \begin{bmatrix} A + B_u D_C C_y & B_u C_C \\ B_C C_y & A_C \end{bmatrix} x_{cl} + \begin{bmatrix} B_w + B_u D_C D_{yw} \\ B_C D_{yw} \end{bmatrix} w \tag{5.13}$$

$$z = \begin{pmatrix} C_z + D_{zu} D_C C_y & D_{zu} C_C \end{pmatrix} x_{cl} + \left(D_{zw} + D_{zu} D_C D_{yw}\right) w \tag{5.14}$$

5.1 H_∞ Control

There are numerous mehods to find an H_∞ output feedback controller. To find a solution of such H_∞ methods, there are several mathematical methods that may be used, such as Riccati equations, linear matrix inequalities or Youla Kucera methods. In this work, an H_∞ synthesis which is given by Doyle *et al.* in 1989 is used by finding a Riccati solution of Hamiltonian matrices. [39]

Control methods H_∞ and H_2 are examined under Hardy spaces however mathematical spaces ar not covered in this work. H_∞ norm is mentioned before the H_∞ control and synthesis.

5.1.1 H_∞ Norm of a System

H_∞ norm of a system can be defined as the peak gain of the system in all frequencies. Consider a system with the system equations**:**

$$\dot{x} = Ax + \sum_{i=1}^{m} B_i \omega_i \tag{5.15}$$

$$y = \sum_{j=1}^{p} c_j x \tag{5.16}$$

$$\omega_i(t) = a_i sin(\omega t + \varphi_i) \qquad \forall\, i = 1, 2, \dots, m \tag{5.17}$$

where m represents the number of inputs and y is written with respect to the number of outputs. In my case, m and p are equal to 2.

Also consider a transfer function as:

$$G_i(s) = C(sI - A)^{-1} B_i \tag{5.18}$$

$$Y(s) = G_i(s) W_i(s) \tag{5.19}$$

where $W_i(s)$ is the reference variable. With an input function as:

The H_∞ norm is the maximal possible vector amplification of this system and given by:

$$\|G(\cdot)_\infty\| = \frac{\sup(\sum_{i=1}^{p}|Y_k(j\omega)|^2)}{\sup(\sum_{i=1}^{m}|W_i(j\omega)|^2)} = sup\bar{\sigma}\{G(j\omega)\} \tag{5.20}$$

where $\sup(.)$ denotes the supremum value and $\bar{\sigma}$ denotes the singular value. In an H_∞ control application, the aim is to reduce this supremum gain value of the system.

5.1.2 $\mathbf{H}_\infty$ Controller

The desired H_∞ controller minimizes this H_∞ norm ($\|G\|_\infty$) lower than a gamma value (γ). For a solution to exist, the following assumptions must be satisfied (see 5.6 and 5.7 for plant and controller notations):

- $(\mathrm{A}, \mathrm{B_u})$ is stabilizable and $(\mathrm{C_y}, \mathrm{A})$ is detectable,
- $(\mathrm{A}, \mathrm{B_w})$ is stabilizable and $(\mathrm{C_z}, \mathrm{A})$ is detectable,
- $\mathrm{D}_{12}'\mathrm{D}_{12}$ and $\mathrm{D}_{21}\mathrm{D}_{21}'$ are in full rank,
- $\begin{bmatrix} \mathrm{A} - \mathrm{j}\omega\mathrm{I} & \mathrm{B_u} \\ \mathrm{C_z} & \mathrm{D}_{12} \end{bmatrix}$ has full column rank for all $\omega \in \mathbb{R}$.
- $\begin{bmatrix} \mathrm{A} - \mathrm{j}\omega\mathrm{I} & \mathrm{B_w} \\ \mathrm{C_y} & \mathrm{D}_{21} \end{bmatrix}$ has full column rank for all $\omega \in \mathbb{R}$.

After they are ensured, two Hamiltonian matrices are defined in order to find an H_∞ controller:

$$H := \begin{bmatrix} A & \gamma^{-2}B_uB_u' - B_wB_w' \\ -C_z'C_z & -A' \end{bmatrix} \tag{5.21}$$

$$J := \begin{bmatrix} A' & \gamma^{-2}C_z'C_z - C_y'C_y \\ -B_uB_u' & -A \end{bmatrix} \tag{5.22}$$

At this point, a linear matrix inequality approach may be used by using semi definite programming (SDP). These linear matrix inequalities are acquired by multiplying these

matrices, H and J, with a convergence matrix, then calculating iterations with respect to the examined synthesis.

As for the Riccati method, Riccati solutions of these Hamiltonian matrices are found. Then a controller may be designed by using the solutions:

$$H \in dom(Ric) \; and \; X \coloneqq Ric(H) \geq 0 \tag{5.23}$$

$$J \in dom(Ric) \; and \; Y \coloneqq Ric(J) \geq 0 \tag{5.24}$$

$$\rho(X_\infty, Y_\infty) < \gamma^2 \tag{5.25}$$

where $dom(.)$ denotes the domain of a function, Ric denotes Riccati equation and ρ is the spectral radius . γ determines the stopping criteria of the iteration algorithms. As these conditions are ensured, the controller is given by:

$$K = \begin{bmatrix} A_\infty & -Z_\infty L_\infty \\ F_\infty & 0 \end{bmatrix} \tag{5.26}$$

where,

$$A_\infty \coloneqq A + \gamma^{-2} B_1 B_1' X_\infty + B_2 F_\infty + Z_\infty L_\infty C_2 \tag{5.27}$$

$$F_\infty \coloneqq -B_2' X_\infty \tag{5.28}$$

$$L_\infty \coloneqq -Y_\infty {C_2}' \tag{5.29}$$

$$Z_\infty \coloneqq (I - \gamma^{-2} Y_\infty X_\infty)^{-1} \text{ [39]} \tag{5.30}$$

H_∞ controllers are designed with this synthesis by using MATLAB's *'hinfsyn'* function. Hinfsyn function gives an oppurtunity to adjust the minimum value of γ. By adjusting that value, we can prevent the control signal to reach high saturation values. The stopping criteria of the iteration algorithm is adjusted by choosing the relative distance. *'hinfsyn'* uses

the γ-iteration bisection algorithm. Bisection, γ-iteration bisection and stopping criteria are mentioned below.

Bisection method — In a simple bisection algorithm, a curve is split into two equal parts. Then, the parts are tested to see in which part the solution lies. Then the chosen part is once again divided by two and the process is repeated.

A γ-iteration bisection algorithm finds the desired γ value with the following receipt:

Step 1 - Initially $[\gamma_l \quad \gamma_u]$ gamma matrix is defined with $\gamma_l > \bar{\sigma}(D)$.

Step 2 - If $(\gamma_u - \gamma_l)/\gamma_l \leq \epsilon$, the given error (or tolerance), stop; $\|G\|_\infty \sim (\gamma_u - \gamma_l)/2$. Otherwise go to the next step,

Step 3 - Set $\gamma = 1/2(\gamma_l - \gamma_u)$ and compute H_γ

Step 4 - Compute the eigenvalues of H_γ

Step 5 - If $\wedge(H_\gamma) \cap \mathbb{C}^0$ set $[\gamma_l \quad \gamma]$ and go back to step 2, else set $[\gamma \quad \gamma_{max}]$ and go back to step 2.

The stopping criteria of the bi section algorithm requires a relative difference value between the last γ value that failed and the last γ value that passed to be less than a previously chosen relative error tolerance, ϵ.

This iteration continues until the two hamiltonian matrices, H and J (5.15,5.16) satisfy the conditions which are shown in 5.1.2. They must not have imaginary values; the stabilizing Riccati solutions of the Hamiltonian matrices, X_∞ and Y_∞ must exist and be positive and semi-definite; the spectral radius of (X_∞, Y_∞) should be less than or equal to γ^2. Variables X_∞ and Y_∞ are then used to calculate the controller equations regarding the synthesis. The state space representations of the models and their controllers are given in the appendix.

The H_∞ controllers are calculated as explained above. The procedure of the simulations and the results are given below.

5.2 H_∞ Controllers and Simulations

In this part, controllers are calculated for the models, mathematical model, tuned mathematical model and N4S4. The main aim of the controllers is reducing the peak values of the gains on every frequency value. These gains represent the gains between the road disturbance and upper mass acceleration which effects passenger comfort.

Passenger comfort is affected by some factors. These factors are, sitting posture, muscle tension, contact points between seat and operator (such as backrests), seat cushion and vibrations transmitted through the seat. Especially for heavy vehicles, the suspension's operating in the low frequency range creates large magnitudes of displacement. It gets increasingly discomforting in even lower ranges of frequencies lower than 20Hz. Therefore frequencies lower than 10Hz are the most practically studied frequencies. Frequencies between 3.5-8Hz are the frequencies which are the most dangerous frequencies for human skeletal health. [15]

In past decades, low back pain was one of the most studied health concern. Passenger movement may be examined on three-axis. Speaking of the vertical movement, the passengers experience a low-back pain under effect around 5Hz regardless of sitting posture. Lower backbones consist of coccyx and lumbar vertebrae, which are the six lowest bones of the human spine. There occurs a transmissibility peak at the third lumbar vertebra. Studies also reveal that when the peak frequency, which is the peak amplitude that's transmitted to the spine, gets lower with less stiff cushions and gets higher with stiffer cushions. [15]

This figure (Figure 5.2) is the SIMULINK design (Figure 5.1-5.2) of the following simulations. With this setup active and passive systems are easily compared.

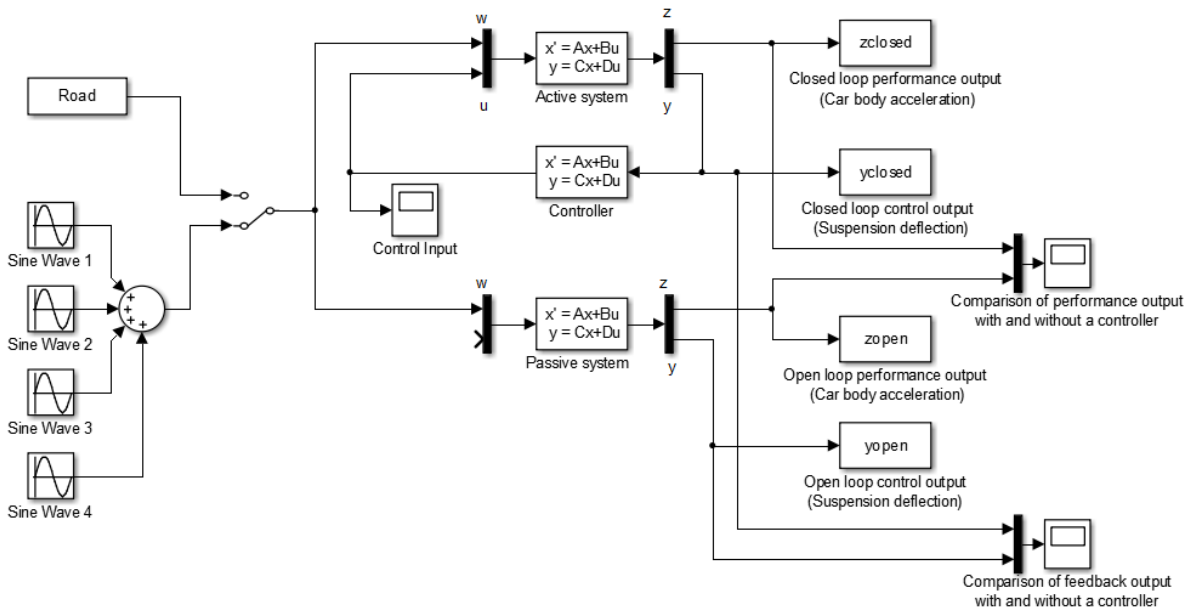

Figure 5.2 Simulation system

For suspension systems, general inspected frequencies are between around 10-100 rad/s as mentioned before.

In order to emphasize the achievement of the controllers, the simulations are ran for different road profiles. The profiles are created by randomized sine-sum of twenty sine-waves. The input amplitudes are adjusted as such for the road displacement to be around 4-5 centimeters (Figure 5.3). It gives a satisfactory test road surface. Former simulations and experiments are done with the first input (cyan input) and the latter simulations are done with the second input (magenta input).

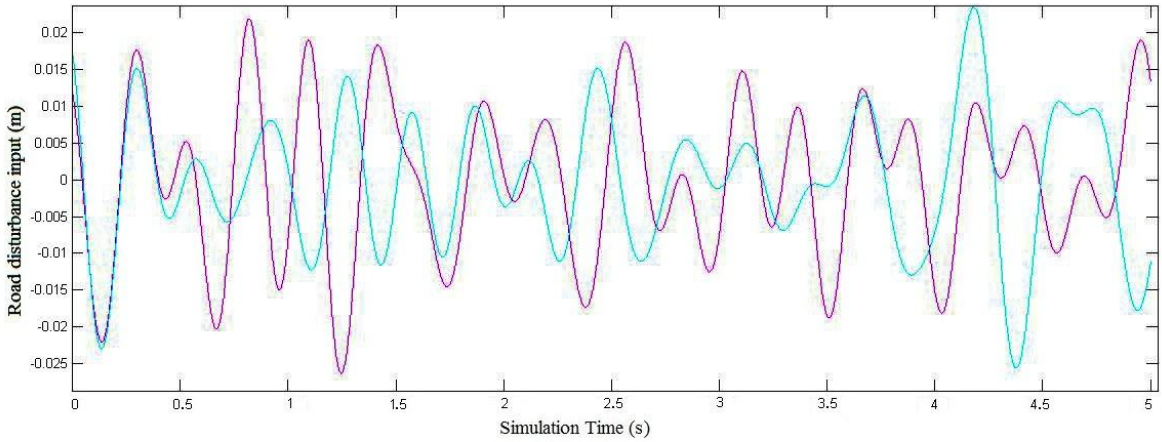

Figure 5.3 Inputs that are used in the simulations (cyan – first input, magenta – second input)

5.2.1 $\mathbf{H}_\infty$ Control and Simulation of the Mathematical Model

An H_∞ controller is designed for the pure mathematical model with respect to the reviewed synthesis by using the Riccati equations of the Hamiltonian matrices (see Appendix-a). Systems infinity norm is reduced from 11181 to 2924. These values are too high as also expected from the mathematical model. The simulations are ran by using above explained randomized twenty sine-sum inputs. The results of upper mass deflection, acceleration and control signal for the first simulation are given in Figure 5.4-5.6.

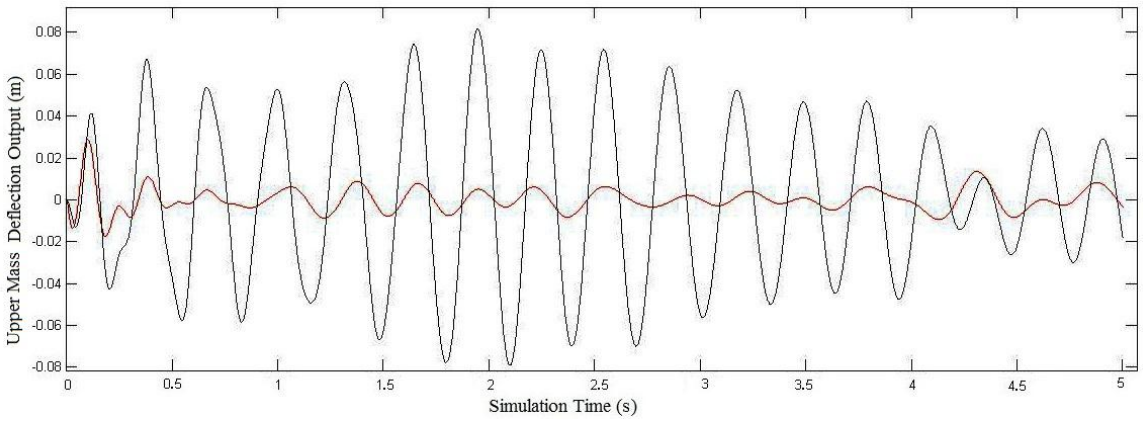

Figure 5.4 Mathematical model, first input – upper mass deflection output (black – open loop, red – closed loop)

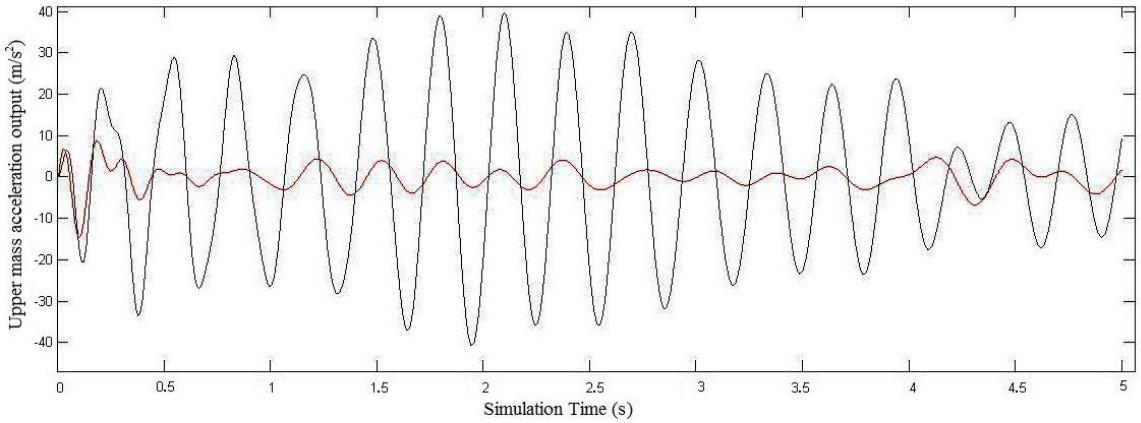

Figure 5.5 Mathematical model, first input – Performance output (black – open loop, red – closed loop)

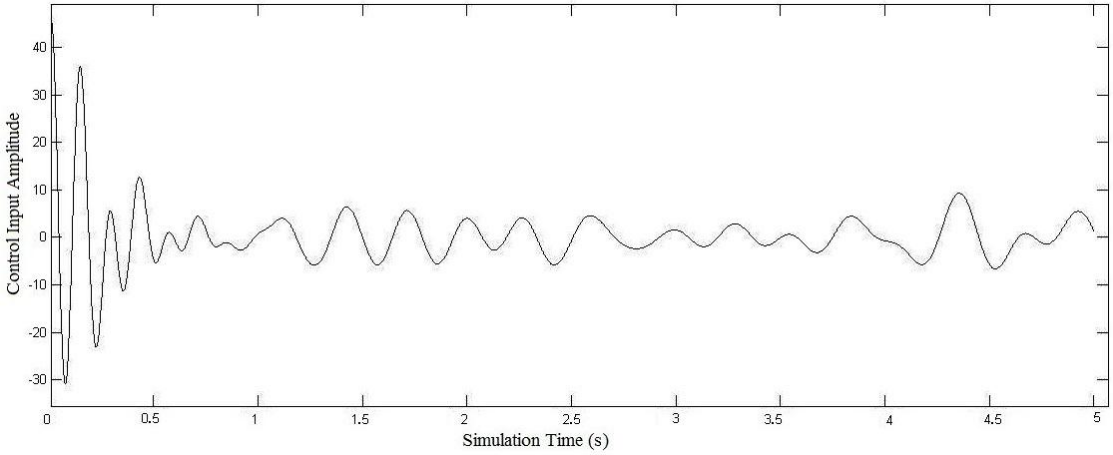

Figure 5.6 Control signal of the first simulation of the mathematical model

The second simulation is done with the second input for the same model, upper mass deflection, acceleration and control signal results are given in Figure 5.7-5.9.

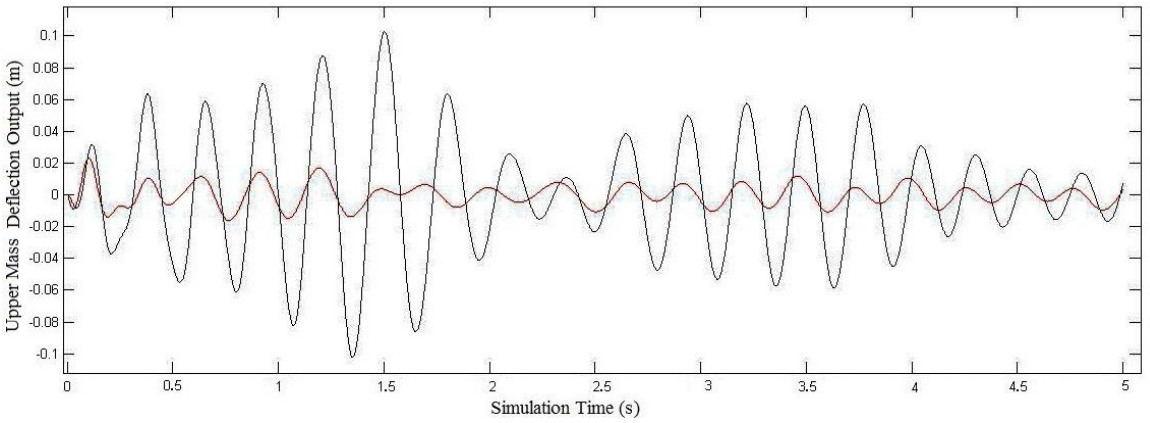

Figura 5.7 Mathematical model, second input – upper mass deflection output (black – open loop, red – closed loop)

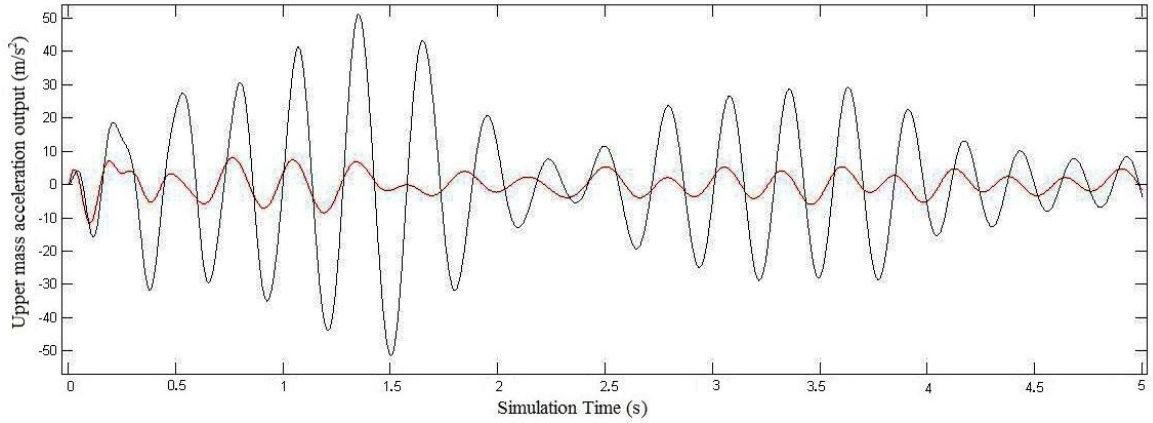

Figure 5.8 Mathematical model, second input – Performance output (black – open loop, red – closed loop)

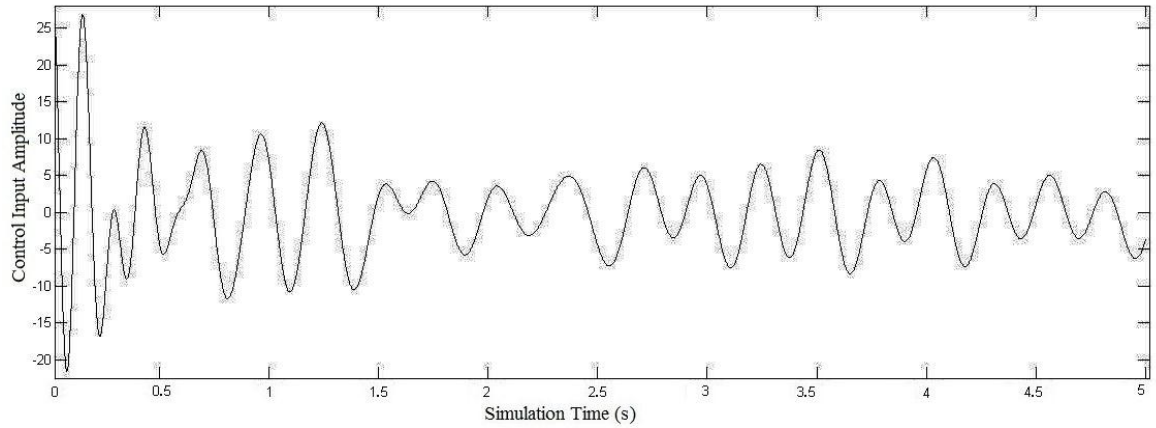

Figure 5.9 Control signal of the second simulation of the mathematical model

Examining the two experiments, it can be said that they are consistent with each other and there is a noticeable improvement on the performance output. However the controller of the mathematical model cannot be applied in the real system because the control input amplitude values reach very high levels to be used in the real system.

5.2.2 $\mathbf{H}_\infty$ Control and Simulation of the Tuned Mathematical Model

An H_∞ controller is designed for the tuned mathematical model again with respect to the same synthesis and the following simulations are ran by using the same inputs shown in Figure 5.3 (See Appendix-b). The system infinity norm is reduced from 18.7455 to 8.4951. Upper mass deflection output, performance output and control signal are given in Figure 5.10-5.12 respectively.

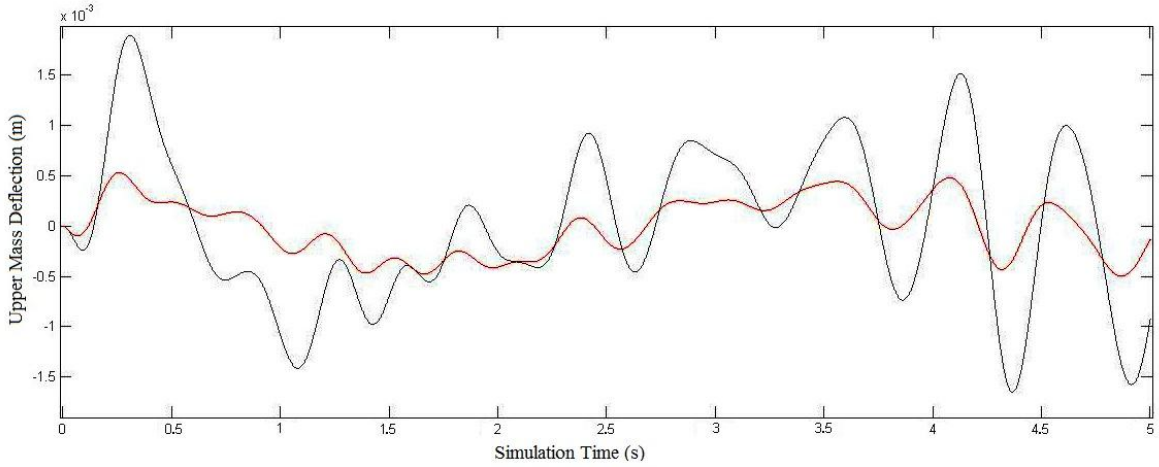

Figure 5.10 Tuned mathematical model, first input – upper mass deflection output (black – open loop, red – closed loop)

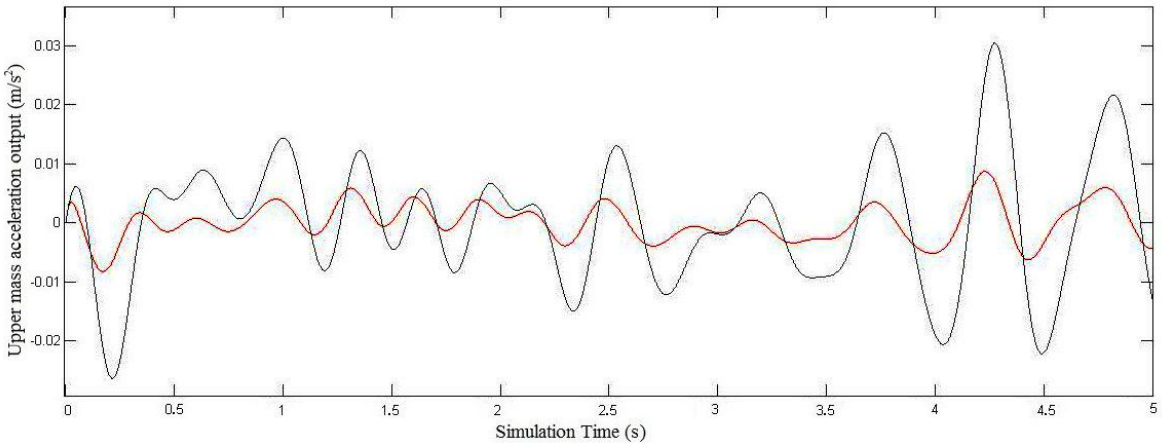

Figure 5.11 Tuned mathematical model, first input – performance output (black – open loop, red – closed loop)

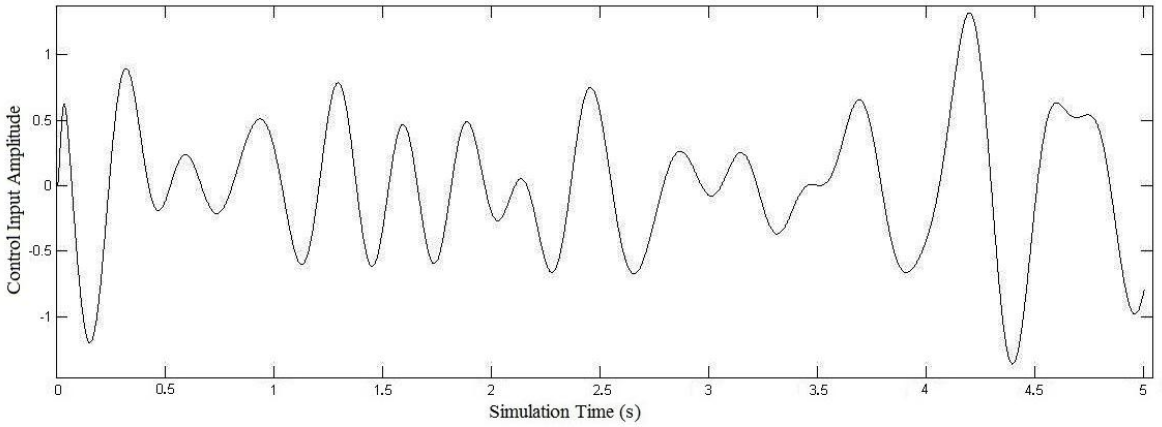

Figure 5.12 Control signal of the first simulation of the tuned model

The second simulation is ran for the tuned mathematical model by using the second input. The upper mass deflection and performance outputs are given in Figure 5.13-5.15.

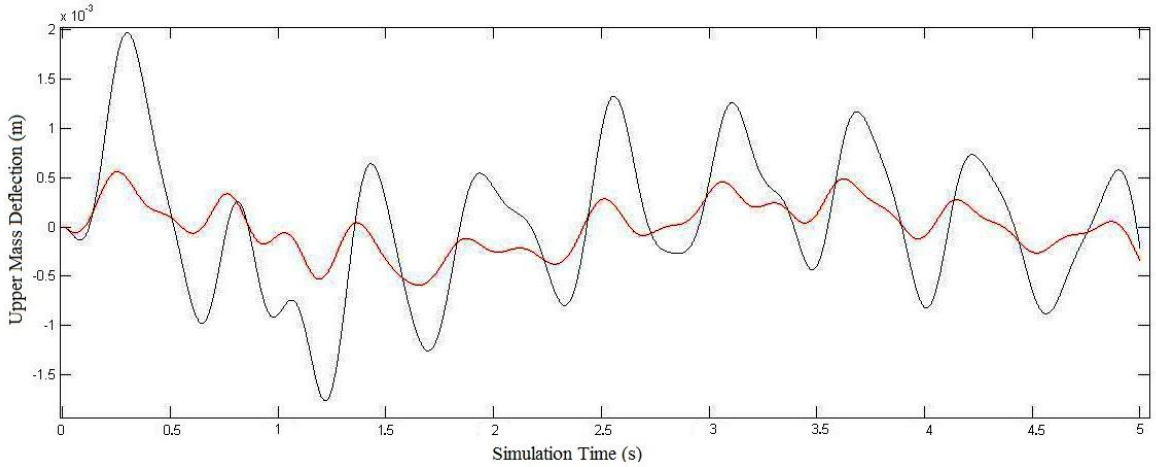

Figure 5.13 Tuned mathematical model, second input – upper mass deflection output (black – open loop, red – closed loop)

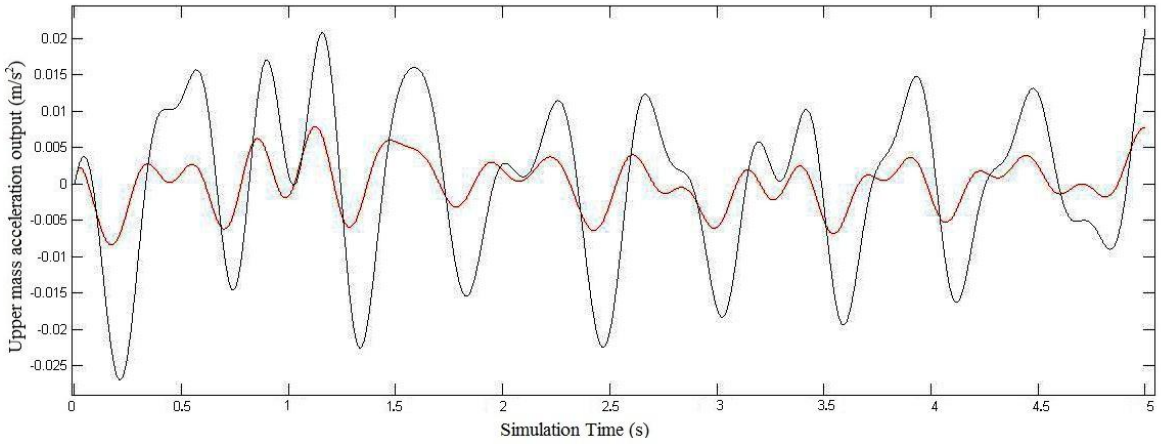

Figure 5.14 Tuned mathematical model, second input – performance output (black – open loop, red – closed loop)

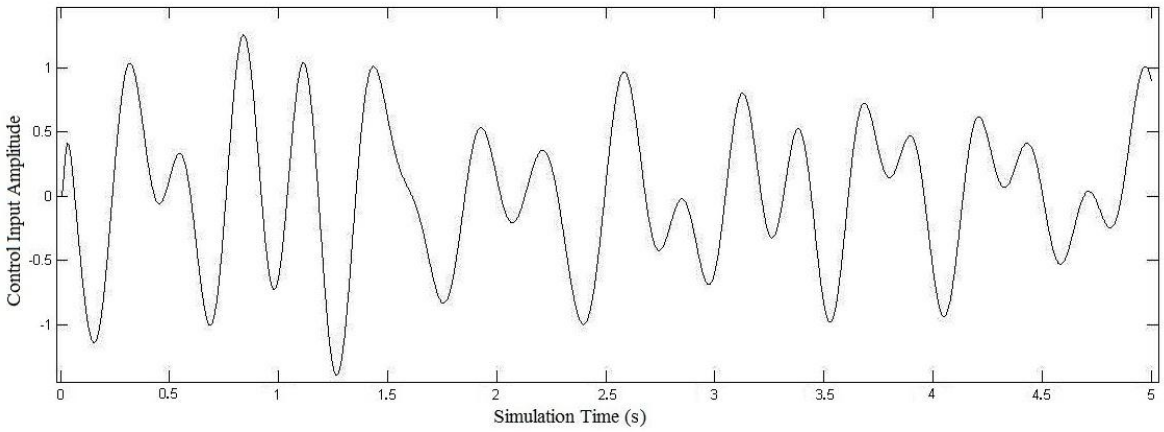

Figure 5.15 Control signal of the second simulation of the tuned model

The results are, again, satisfactory and consistent with each other, the aim is achieved. Control input being low, the actuator saturation limits are ensured. However controller gain is too high to be realized in the real system.

5.2.3 Control and Simulation of the n4s4 System Identification Model

The controller of the N4S4 model is calculated with the control technique given by the study [41] (see Appendix-c). In this technique, H_∞ norm values are minimized by placing the pools in a chosen zone. This way the pools are placed in the left side of -2 real value in a circle with radius:150 [37].

At this point, a band-pass filter is designed for the frequencies between 4-8 Hz. This way our controller is more effective on these frequencies. Since it is second degree, our closed loop system becomes a sixth order system.

The main aim is making the dynamic response faster while preventing the control output saturation. The infinity norm is reduced from 38.9257 to 18.6001. The simulations are done with the same twenty sine-sum inputs with random amplitudes and frequency values. The upper mass deflection output, performance output and the control signal are given in Figure 5.15-5.17 respectively.

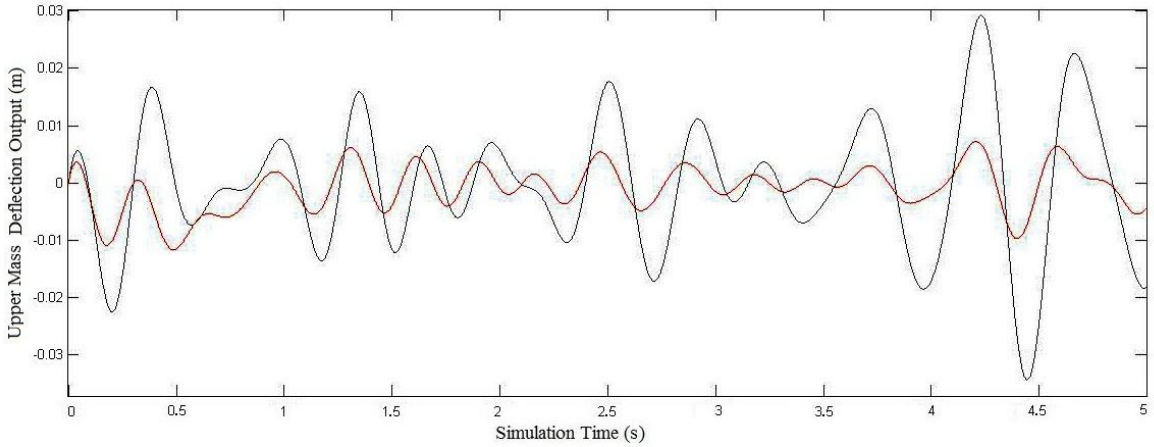

Figure 5.16 N4S4 model, first input – upper mass deflection output (black – open loop, red – closed loop)

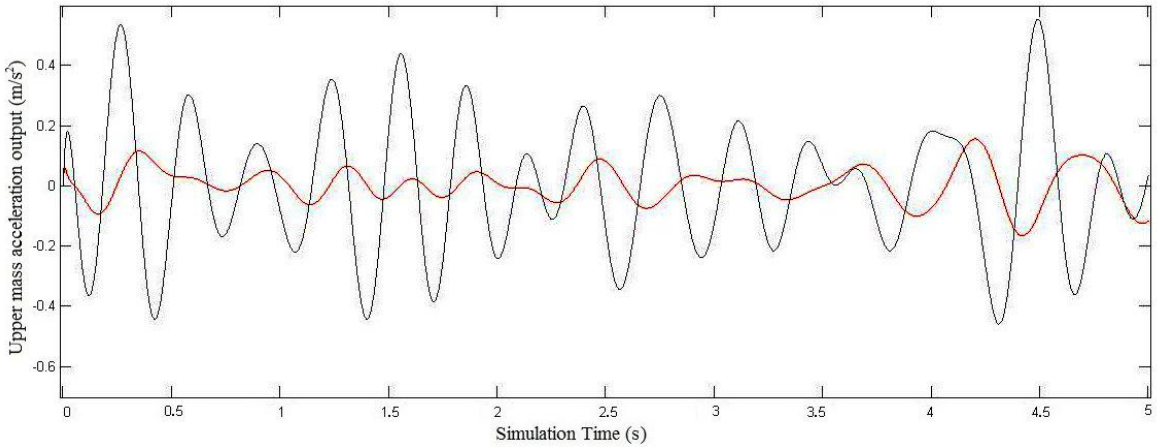

Figure 5.17 N4S4 model, first input – performance output (black – open loop, red – closed loop)

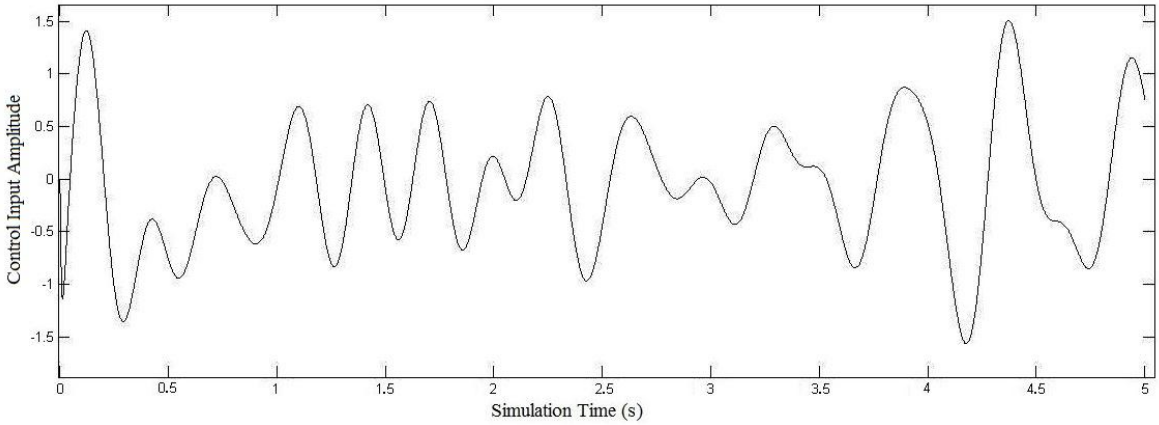

Figure 5.18 Control signal of the first simulation of the N4S4 model

The simulation is ran again by using the second input. The upper mass deflection, performance output and control signal values are given in Figure 5.19-21, respectively.

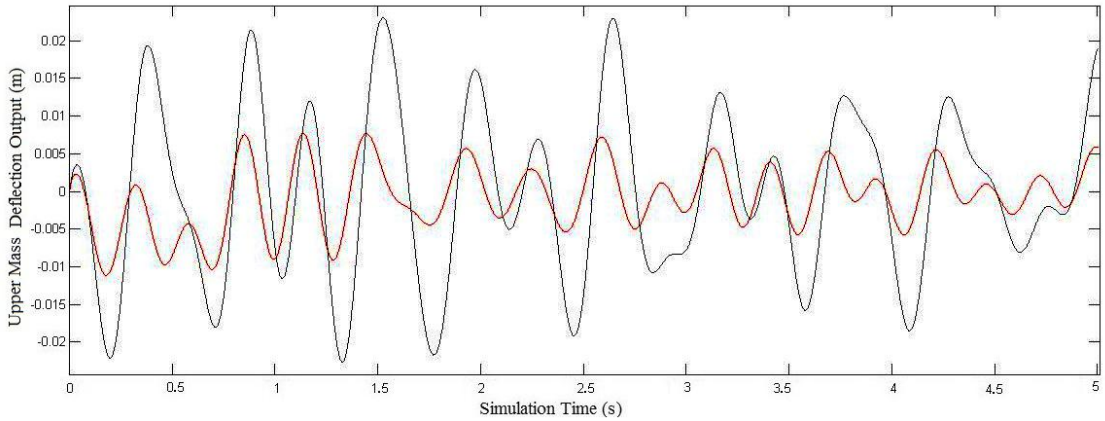

Figure 5.19 N4S4 model, second input – upper mass deflection output (black – open loop, red – closed loop)

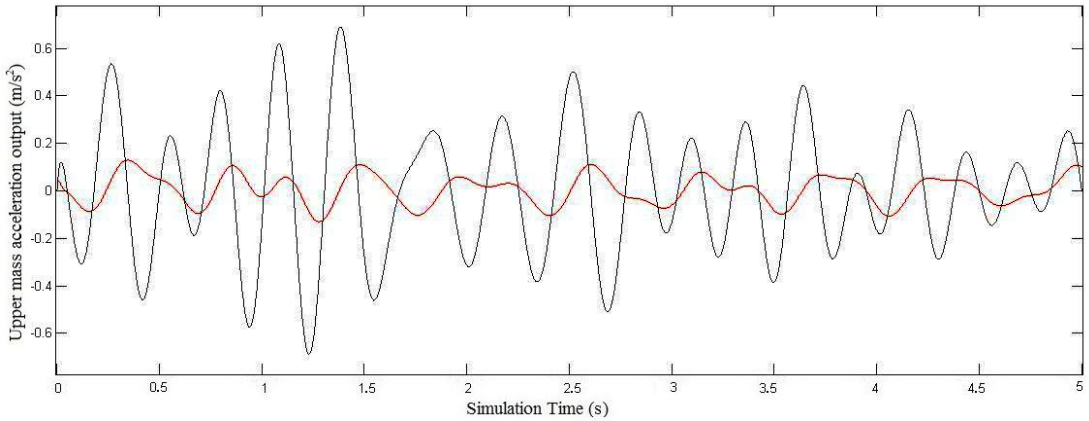

Figure 5.20 N4S4 model, second input – performance output (black – open loop, red – closed loop)

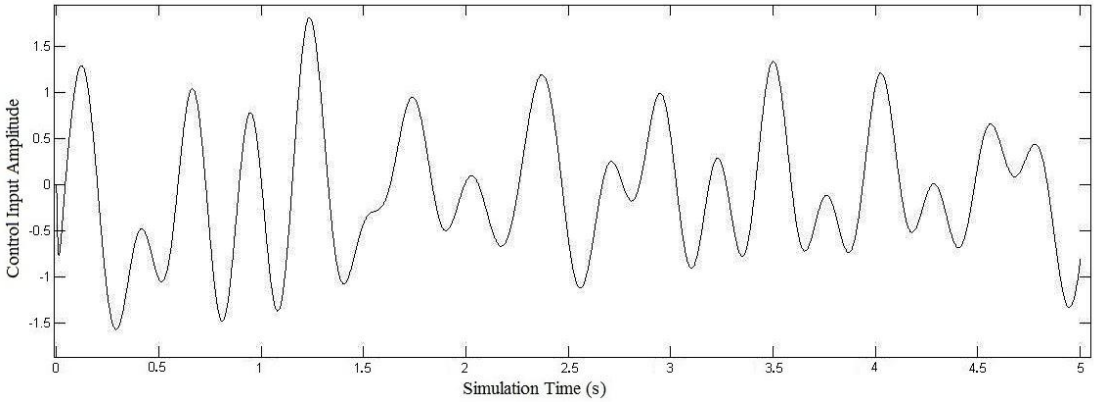

Figure 5.21 Control signal of the second simulation of the N4S4 model

Fortunately control input amplitudes do not override system actuator's psychical limits. The controller can be tested on the real system.

It can be seen that the H_∞ norm is reduced. The aim is obtained in the simulations. Hereon, the N4S4 controller is tested by using it on the real system.

5.3 H_∞ Control Experiments on the Real System

The controller of the N4S4 model is entered on the real system. The experiments are done by using the same inputs in order to be able to make a comparison. The results of the upper mass deflection output, performance output and control signal are given in Figure 5.22-5.24 respectively for the first experiment with the first input.

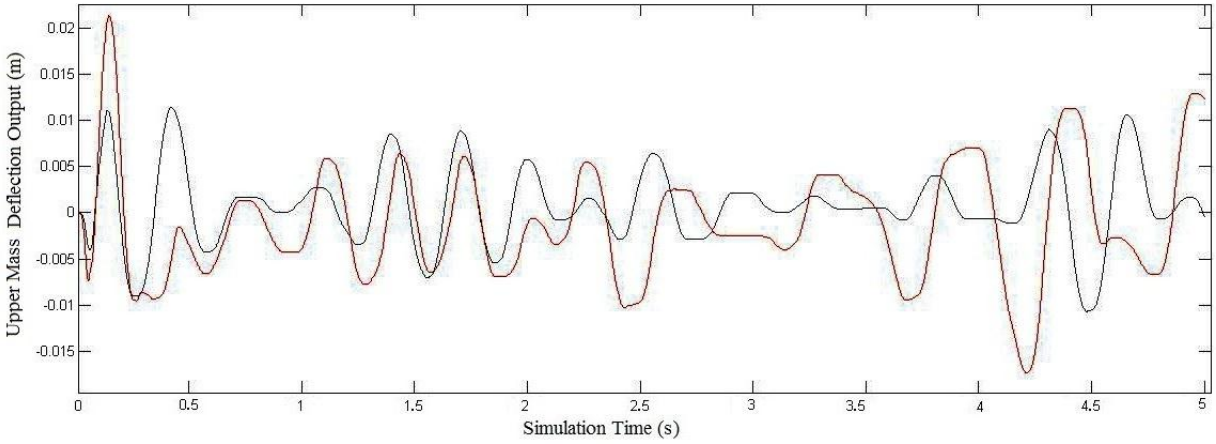

Figure 5.22 Real system, first input – upper mass deflection output (black – open loop, red – closed loop)

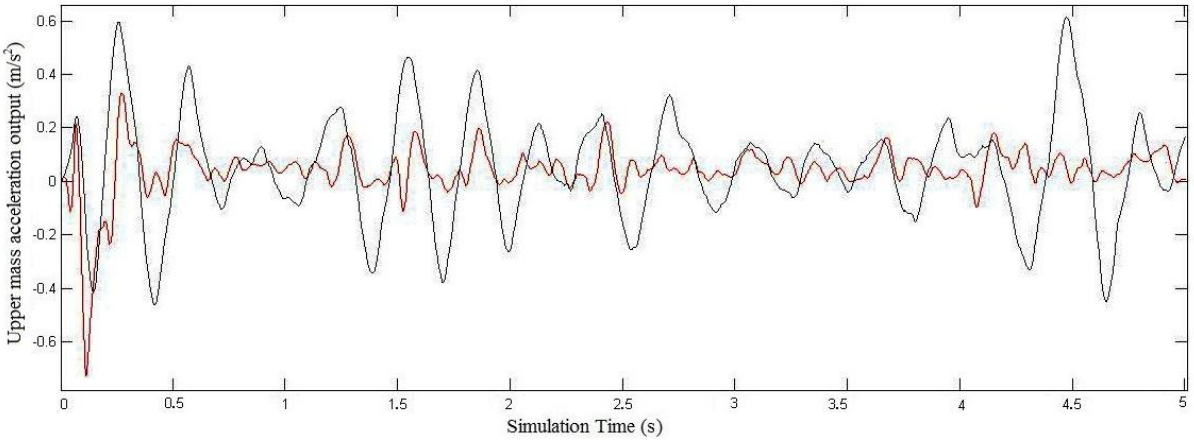

Figure 5.23 Real system, second input – performance output (black – open loop, red – closed loop)

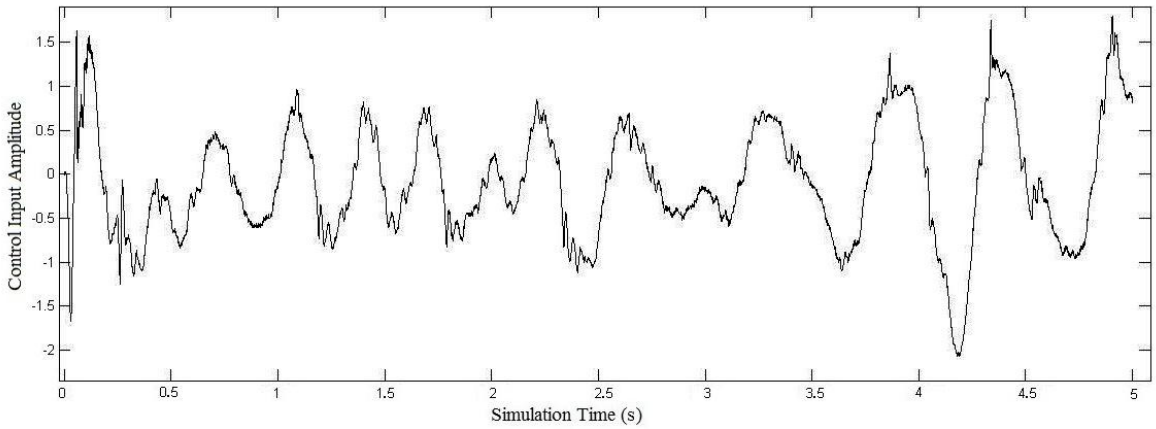

Figure 5.24 Control signal of the first experiment on the real system

The second experiment is done again by using the second input, upper mass deflection output, performance output and control signal results are given in Figure 5.25-5.27 respectively.

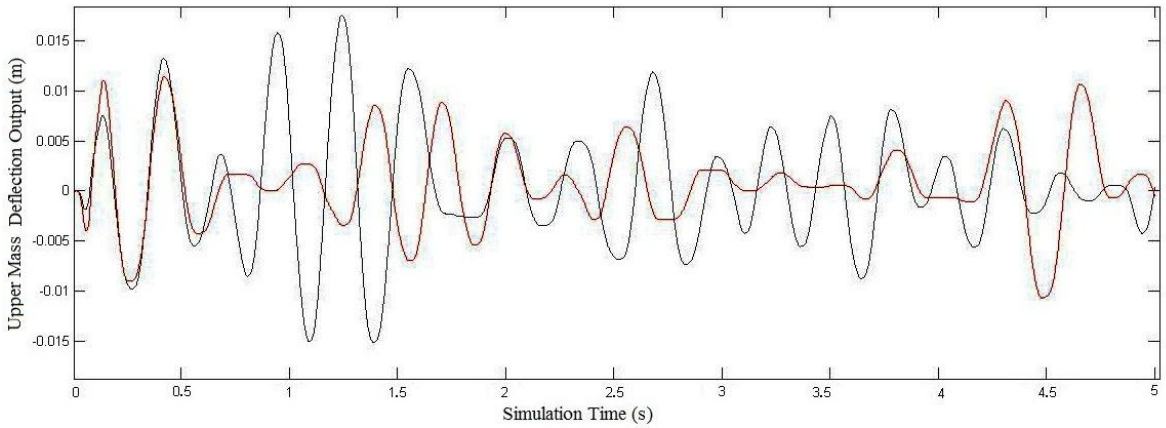

Figure 5.25 Real system, first input – upper mass deflection output (black – open loop, red – closed loop)

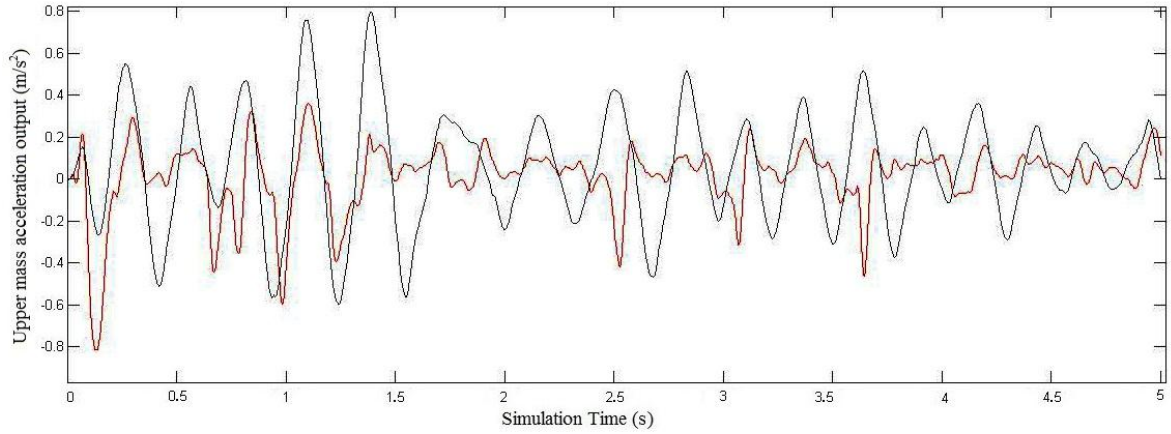

Figure 5.26 Real system, second input – performance output (black – open loop, red – closed loop)

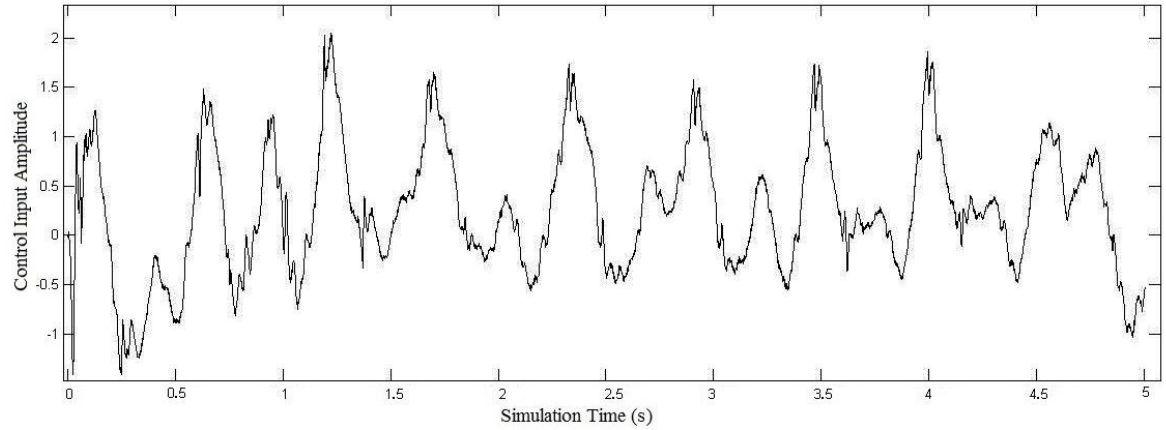

Figure 5.27 Control signal of the second experiment on the real system

As also seen in the figures, even though our main aim is to reduce the effects of the road to the upper mass acceleration, there is a remarkable improvement in the upper mass deflection values. Both experiments are again consistent with each other and the H_∞ norm of the upper mass acceleration performance output is reduced from 0.72 to 0.33.

CHAPTER 6

RESULTS AND DISCUSSION

6.1 Results

In the second chapter, some existent suspension models are inspected before working on the real system model. Mathematical models of different suspension systems are given and the basic information and characteristics of the elements of an active suspension system are given. Then the mechanical characteristics of the real system are inspected. In the light of these characteristics and concepts several mathematical models are found by Lagrange and Newton modeling methods. As working on the system, it is seen that the known parameters are different than the real ones. Non parametric system identification methods are included at this point and the parameters are tuned and compared with the previous ones with non parametric techniques (Chapter 4). The non parametric techniques include examining the frequency spectrum of the system in various frequencies. The validity of the modified model is secured by checking the results of the pure mathematical model. In addition to the modification of the mathematical model, the well-known parametric system identification techniques are also used to find a better fitting model by using MATLAB system identification toolbox. A fourth order state space system (N4S4), is found by this way. It is shown in Chapter 4 that the N4S4 model describes the system accurately. In Chapter 5, the H_∞ control theory is briefly explained and some H_∞ controllers are designed by the H_∞ synthesis given by Doyle *et al.,* in 1989. By the virtue of the H_∞ controller, the closed loop system peak gain, which is between the road disturbance input and performance output is reduced to the minimum value.

The H_∞ controllers are calculated for the mathematical model and tuned mathematical model and tested in SIMULINK. H_∞ controller is calculated with respect to a pole placement study given by [41]. N4S4 system identification model Some related works are examined in order to obtain a realistic test road profile and two road profiles are then created by summing twenty random sine-waves [14]. The road disturbance inputs are different yet similar. The performance of these H_∞ controllers are tested, the results are given and compared. As the control signals are examined, it is seen that the control signals for the tuned mathematical model and the N4S4 model are in the saturation limits of the actuator. Between the two, the performance of the N4S4 controller is higher and it is decided to be tested on the real system.

Before beginning the real system experiments , the system is altered by adding a filter to the performance output. Thus it has a more realistic behaviour. The final results are obtained by this way. Adding the second order band pass filter to our system makes it sixth order. The H_∞ norm is confirmed to be reduced in the final results.

6.2 Discussions

In the modeling section of this work, we discussed beneficial sides of non parametric and parametric techniques. The researchers choose such techniques with respect to the application area. In the light of the previous discussions, we may conclude the following claims:

- The tuned model may be further improved by making different interpretations with the non-parametric identification techniques.
- The strongest restriction of the N4S4 model is encountered designing the controller. The states are not explicit for this model. Only a controller with output feed-back scheme can be designed which is considered in this work.
- If the mathematical model is observable, non-measurable states can be easily predicted by an observer. The knowledge on dynamic system states is a valuable tool for designers. A static state feedback scheme can be utilized easily with such

tools. This way the obtained controller is constructed as zero-order, making it more durable against noises; also it is easier to be applied for the real system.

- It is seen that the appropriate controller for the N4S4 and the closed loop system (with weighted filter) are sixth order. Therefore the closed loop system has twelfth order which may cause some problems and difficulties such as blow-up, in real life applications.

For a future work, a low-order output feedback controller design may be considered. This way while the applicability level of the controller is getting higher, performance sacrifice is being kept low. In addition to this future work, we may extend the philosophy on the design process. Here, upper mass acceleration is only taken into consideration as a performance criterion, which means improving the passenger comfort. However, we may use the handling and driving safety criterion for the performance criteria too. For another future work, a low-order controller which provides a sub-optimal level for multi-objective optimization problem can be designed.

REFERENCES

[1] Smith, J.H., (2001). An Introduction to Modern Vehicle Design, Elsevier.

[2] Rajamani, R., (2012). Vehicle Dynamics and Control, Second Edition, Springer.

[3] Lu, H.Y., (2006). Dynamic Model and Control of Vehicles, Master's Thesis, Lakehead University, Ontario.

[4] Els, P. S., (2016). The Ride Comfort Vs. Handling Compromise for Off-road Vehicles, Doctoral Thesis, University of Pretoria Faculty of Engineering, Pretoria.

[5] Chen, Y., (2009). "Skyhook Surface Sliding Mode Control on Semi-Active Vehicle Suspension System for Ride Comfort Enhancement.", Engineering, 1: 23-32.

[6] Xue, X. D., Cheng, K. W., Zhang, Z., Lin, J. K., Wang, D. H., Bao, Y. J., Cheung, N. (2011). "Study of Art of Automotive Active Suspensions." Power Electronics Systems and Applications (PESA), 2011 4th International Conference, Hong Kong.

[7] Hrovat D. (1997). "Survey of advanced suspension developments and related optimal control applications.", Automatica, 33: 1781-1817.

[8] Sharp, R. S., Crolla, D. A. (1987). "Road Vehicle Suspension System Design - a review",Vehicle System Dynamics, 16: 167-192.

[9] Ljung, L., (1999). System Identification: Theory For The User, Second Edition, Prentice Hall, Upper Saddle River..

[10] Els, P.S., (2006). The Ride Comfort vs. Handling, Doctoral Thesis, University of Pretoira Faculty of Engineering, Pretoria.

[11] Lopez, S.L., (2010). Optimal H_∞ Design of Casuel Multirate Controllers and Filters, Doctoral Thesis, University of California, Irvine.

[12] Amirifar, R., Sadati, N., (2005)."A Low-Order H_∞ Controller for an Active Suspension System via Linear Matrix Inequalities", Journal of Vibration and Control, 10: 1181.

[13] Chen, H., Guo, K.H., (2005). "Constrained H_∞ Control of Active Suspensions: An LMI Approach", IEEE Transactions on Control Systems Technology, 13: 3.

[14] Gadewadikar, J., (2007). H-Infinity Output-Feedback Control: Application to Unmanned Aerial Vehicle, Doctoral Thesis, Faculty of Graduate School of The University of Texas, Arlington

[15] Kumar, S., (2007). Biomechanics in Ergonomics, Second Edition, CRC Press.

[16] Tong, R.T., (2001). Ride Control - A Two-State Design For Heavy VehicleSuspension, Doctoral Thesis, Graduate Collage of University of Illinois, Chicago.

[17] Cao, J., Honghai, L., Li, P. J., Brown, D. (2008). "State of the Art in Vehicle Active Suspension Adaptive Control Systems Based on Intelligent Methodologies.", IEEE TRANSACTIONS ON INTELLIGENT TRANSPORTATION SYSTEMS, 9: 3.

[18] Balachandran, B., Magrab, E. B. (2008). Vibrations, Cengage Learning, Boston.

[19] Schmitz, T. L., Smith, K. S. (2012). Mechanical Vibrations: Modeling and Measurement, Springer, New York City.

[20] Bottega, W. J., (2006). Engineering Vibrations, CRC Press, Boca Raton.

[21] Wikipedia, Damping, http://upload.wikimedia.org/wikipedia/commons/f/fd/Damping_1.svg , 25 February 2014.

[22] Sciulli, D, (1997). Dynamics and Contro for Vibration Isolation Design, Doctoral Thesis, Faculty of Virginia Polytechnic Institute, Virginia.

[23] Kelly, S. G. (2000). Fundamentals of Mechanical Vibrations, McGraw-Hill Education, New York City.

[24] Ogata, K. (2009). Modern Control Engineering, Prentice Hall, Upper Saddle River.

[25] Ambekar, A.G., (2007). Mechanism and Machine Theory, Prentice-Hall of India Private Limited, New Delhi.

[26] Pope, J. E. (1996). "Rules of Thumb for Mechanical Engineers.", Gulf Publishing Company, Houston.

[27] Sinha, A. (2010). Vibration of Mechanical Systems, Cambridge University Press, Cambridge.

[28] Johnson, T. J., (2002). Analysis Of Dynamic Transmissibility As A Feature For Structural Damage Detection, Master's Thesis, Faculty of Purdue University, West Lafayette.

[29] Kovačić, I., Milovanović Z., Brennan M. J., (2008). "On the Relative and Absolute Transmissibility of a Vibration Isolation System Subjected to Base Excitation", Working and Living Environmental Protection, 5: 39-48.

[30] Abouel-Nour, A.M.A.A.R., (1989). Active Control of Vehicle Suspensions, Doctoral Thesis, The University of Leeds, Leeds.

[31] Kruzcek, A., Stribrsky, A. (2004). "A Full-Car Model for Active Suspension – Some Practical Aspects.", Mechatronics, 2004 ICM '04, 3-5 June 2004, Istanbul.

[32] Guido, K., Oliver, F., Lohmann, B. (2008). “Potential of Low Bandwidth Active Suspension Control with Continuously Variable Damper.” Proceedings of the 17th World Congress The International Federation of Automatic Control, 06-11 July, Seoul.

[33] Ljung, L., (2014). System Identification Toolbox For Use with MATLAB, http://www.mathworks.com/help/pdf_doc/ident/ident_gs.pdf, 3 March 2014.

[34] Huckle, T.K., (2008). “Compact Fourier Analysis for Designing Multigrid Methods”, SISC 31:1.

[35] Ljung, L., (2004). Practical Issues of System Identification, http://www.eolss.net/EolssSampleChapters/C05/E6-43-12/E6-43-12-TXT.aspx, 27 July 2014.

[36] Overschee, P. V., Moor, B. D. (1992). “N4SID: Subspace Algorithms for the Identification of Combined Deterministic-Stochastic Systems.”, Automatica, 30: 75-93.

[37] Erol B. (2015). Çeyrek Taşıt Aktif Süspansiyon Modeli Çıkarımı ve Kontrolü, Technical University Yildiz, Istanbul.

[38] Dahleh, M., Dahleh, M. A., & Verghese, G., (2011). Lectures on Dynamic Systems and Control. http://ocw.mit.edu/courses/electrical-engineering-and-computer-science/6-241j-dynamic-systems-and-control-spring-011/readings/, 23 May 2014.

[39] Doyle, J.C., Glover, K., Khargonekar P., Francis B., (1989). "State-space solutions to standard H2 and H∞ control problems," IEEE Transactions on Automatic Control, 34: 831–847.

[40] Skogestad, S., Postlethwaite, I. (2005). Multivariable Feedback Control: Analysis and Design, John Wiley & Sons, Hoboken.

[41] Chilali, Mahmoud, and Pascal Gahinet. (1996). "H∞ Design with Pole Placement Constraints: an LMI Approach." Automatic Control, IEEE Transactions on 41.3: 358-367.

APPENDIX-A

MATHEMATICAL MODEL AND ITS CONTROLLER

Mathematical model state space structure:

A=
[0 0 1 0
0 0 0 1
-500 500 -3 3
333.3 -2333.3 2 -2]

Bw=
[0
0
0
2000]

Bu=
[0
0
1
-0]

C1= [-500 500 0 0]

C2= [1 -1 0 0]

B= [Bw Bu]

C=
[C1
C2]

D=

[0 0
0 0]

The MATLAB code that was used to find the controller:

[K,CL,GAM,INFO] = hinfsyn(P,1,1)

State space structured controller of the mathematical model:

K.a=
[-996.8 996.8 1 0
997.8 -997.8 0 1
-4.769e+05 3.724e+05 -1006 -1.192e+04
1.996e+06 -1.998e+06 2 -2]

K.b=
[996.8
-997.8
-5984
-1.995e+06]

K.c= [-4.824e+05 3.779e+05 -1003 -1.193e+04]

K.d= [0]

APPENDIX-B

TUNED MATHEMATICAL MODEL AND ITS CONTROLLER

Tuned mathematical model state space structure:

A=

```
[     0            0         1.0000        0
      0            0            0         1.0000
  -5.0000    5.0000    -1.3500    1.3500
  10.0000  -20.0000    2.7000   -2.7000  ]
```

B=

```
[   0              0
    0              0
    0          0.0500
  10.0000   -0.1000   ]
```

C=

```
[ -5.0000    5.0000   -1.3500    1.3500
    1.0000   -1.0000        0           0     ]
```

D=

```
[   0     0
    0     0   ]
```

The MATLAB code that was used to find the controller:

```
[K,CL,GAM,INFO] = hinfsyn(P,1,1)
```

State space structured controller of the tuned mathematical model:

K.a=

[-98.63 98.63 1 -0.000367

38.75 -38.75 0.0001081 0.9999

-64.89 98.66 -96.03 55.24

1.012e+04 -1.02e+04 192 -110.4]

K.b =

[420.6

-165.2

-790.8

-4.102e+04]

K.c = [-1151 1309 -444.1 252.7]

K.d = [0]

APPENDIX-C

N4S4 MODEL AND ITS CONTROLLER

N4S4 model state space structure:

A =

[-19.77 25.66 -40.66 26

-4.196 -10.46 -34.72 -39.71

-9.902 -0.6211 -41.41 -11.23

7.581 9.314 23.54 8.804]

B =

[-69.31 0.2581

40.01 0.2074

52.84 0.1746

-29.99 -0.04572]

C =

[19.73 3.805 29.58 -27.52

0.05301 -0.5588 1.233 0.687]

D =

[0 0

0 0]

N4S4 model with the filter:

A=

```
[  -19.77     25.66    -40.66      26         0         0
   -4.196    -10.46    -34.72    -39.71      0         0
   -9.902   -0.6211    -41.41    -11.23      0         0
    7.581     9.314     23.54     8.804      0         0
     78.9     15.22     118.3    -110.1   -27.11    -42.56
        0         0         0         0        32         0  ]
```

B =

```
[    -69.31     0.2581
      40.01     0.2074
      52.84     0.1746
     -29.99   -0.04572
          0          0
          0          0  ]
```

C =

```
[    4.855     0.9365   7.281    -6.773    4.908    -2.619
  0.05301   -0.5588   1.233     0.687       0          0      ]
```

D =

```
[  0     0
   0     0  ]
```

The MATLAB code that was used to find the controller:

[K,CL,GAM,INFO] = hinfsyn(P,1,1)0

State space structured controller of the N4S4 model:

K.a=

```
[  -92.9837   -1.6365     86.1223     31.8634     1.5626    1.3972
```

196.1473 5.1502 -167.5197 -69.9679 -4.6389 -4.9312

-14.4805 10.6889 -70.4462 -22.6472 -2.4327 -1.6763

-1.9922 0.8193 4.1429 -1.4461 5.8888 0.0353

326.3466 57.3257 -538.9062 -202.6529 -11.0149 3.0366

-0.1525 -0.0293 0.2601 0.0918 -0.0119 -108.1223]

K.b =

[123.6929

-286.5754

8.4183

3.0304

-510.4033

0.2380]

K.c = [688.0257 38.5847 -558.8781 -223.4820 -13.3304 -12.8027]

K.d = [-905.1656]

CURRICULUM VITAE

PERSONAL INFORMATION

Name Surname : Canalp BELGÜTAY

Date of birth and place : 1990, Istanbul

Foreign Languages : English, German

E-mail : canalpbelgutay@gmail.com

EDUCATION

Degree	Department	University	Date of Graduation
Master	Control and Automation Engineering	Technical University Yildiz	2015
Undergraduate	Mechanical Engineering	Kocaeli University	2012
High School	Natural sciences	Kartal Anadolu Lisesi	2008

WORK EXPERIENCE

Year	Corporation/Institute	Enrollment
2013-2013	Johnson Controls, Inc. Istanbul (Turkey)	Electronics engineer

AWARDS

1. One month DAAD (The German Academic Exchange Service) scholarship